



**The C2 fragment from *Neisseria meningitidis* antigen NHBA increases endothelial permeability by destabilizing adherens junctions**

Journal:	<i>Cellular Microbiology</i>
Manuscript ID:	CMI-13-0221.R1
Manuscript Type:	Research article
Date Submitted by the Author:	29-Nov-2013
Complete List of Authors:	Casellato, Alessandro; Venetian Institute of Molecular Medicine, Venetian Institute of Molecular Medicine Rossi Paccani, Silvia; Novartis Vaccines & Diagnostics, Microbial Molecular Biology Barrile, Riccardo; Novartis Vaccines & Diagnostics, Microbial Molecular Biology Bossi, Fleur; University of Trieste, Department of Medicine, Surgery and Health Sciences Ciocchi, Laura; Novartis Vaccines & Diagnostics, Microbial Molecular Biology Codolo, Gaia; University of Padova, Department of Biology Pizza, Mariagrazia; Novartis Vaccines & Diagnostics, Microbial Molecular Biology arico, beatrice; Novartis Vaccines & Diagnostics, Microbial Molecular Biology de Bernard, Marina; University, Biology Department
Key Words:	Vaccines, Disease processes, Infection, Microbial-cell interaction

**The C2 fragment from *Neisseria meningitidis* antigen NHBA increases endothelial permeability by destabilizing adherens junctions**

**Running Title:** C2 fragment from NHBA alters endothelial integrity

**Alessandro Casellato<sup>1</sup>, Silvia Rossi Paccani<sup>2</sup>, Riccardo Barrile<sup>2</sup>, Fleur Bossi<sup>3</sup>, Laura Ciocchi<sup>2</sup>, Gaia Codolo<sup>1,4</sup>, Mariagrazia Pizza<sup>2</sup>, Beatrice Aricò<sup>2</sup>, Marina de Bernard<sup>1,4</sup>**

<sup>1</sup>Venetian Institute of Molecular Medicine, Padua, Italy; <sup>2</sup>Novartis Vaccines and Diagnostics, Siena, Italy; <sup>3</sup>Department of Medicine, Surgery and Health Sciences, University of Trieste, Trieste, Italy; <sup>4</sup>Department of Biology, University of Padua, Padua, Italy

**Address correspondence to:**

Prof. Marina de Bernard, Venetian Institute of Molecular Medicine, Via Orus 2, 35129 Padova Italy  
e-mail address: marina.debernard@unipd.it, Phone: +39.049.7923223, Fax: +39.049.7923250 and Dr. Beatrice Aricò, Novartis Vaccines and Diagnostics, Siena, Italy, e-mail address: beatrice.arico@novartis.com, Phone: +39.0577.243239, Fax: +39.0577.539314.

## Summary

*Neisseria meningitidis* is a human pathogen that can cause fatal sepsis and meningitis once it reaches the blood stream and the nervous system. Here we demonstrate that a fragment, released upon proteolysis of the surface-exposed protein Neisserial Heparin Binding Antigen (NHBA), by the bacterial protease NalP, alters the endothelial permeability by inducing the internalization of the adherens junction protein VE-cadherin. We found that C2 rapidly accumulates in mitochondria where it induces the production of reactive oxygen species: the latter are required for the phosphorylation of the junctional protein and for its internalization that, in turn, is responsible for the endothelial leakage. Our data support the notion that the NHBA-derived fragment C2 might contribute to the extensive vascular leakage typically associated with meningococcal sepsis.

1  
2  
3  
4  
5  
6  
7  
8  
9  
10  
11  
12  
13  
14  
15  
16  
17  
18  
19  
20  
21  
22  
23  
24  
25  
26  
27  
28  
29  
30  
31  
32  
33  
34  
35  
36  
37  
38  
39  
40  
41  
42  
43  
44  
45  
46  
47  
48  
49  
50  
51  
52  
53  
54  
55  
56  
57  
58  
59  
60

**Introduction**

*Neisseria meningitidis* is an encapsulated, Gram-negative bacterium that colonizes the nasopharynx of 8-20% of healthy individuals. In a small proportion of infected patients, the bacterium crosses the mucosal barrier and reaches the bloodstream, giving rise to meningitis or fulminant septicaemia. One of the most dramatic features of severe meningococcal sepsis is the occurrence of widespread *purpura fulminans*, in which disseminated intravascular coagulation is associated with massive vascular leakage and multiple organ failure (Pathan *et al.*, 2003).

13 serogroups of *N. meningitidis* have been identified, on the basis of the specific composition of the polysaccharide capsule, and five of them are associated with the disease (Caesar *et al.*, 2013). Although vaccines containing purified polysaccharide antigens are available against four of the five pathogenic serogroups, the capsular polysaccharide of Meningococcus serotype B (MenB) is not suitable for the formulation of human vaccines. Indeed, the MenB strain is characterized by a capsule made of sialic acid, one of the constitutive sugars of the human cellular glycolix. Therefore, sialic acid represents a poorly immunogenic self-antigen in humans that cannot be used for vaccination, thus rendering the strategy adopted for the other strains not suitable for MenB. Novartis Vaccines in 2000 overcame this obstacle by adopting an innovative strategy called reverse vaccinology. This bio-informatics method, combined with molecular biology and biochemical techniques, led to the discovery of a plethora of new MenB conserved antigens potentially considered as vaccine candidates. Among these antigens, is the Neisserial Heparin Binding Antigen (NHBA, elsewhere called GNA2132). In combination with the other components of the Novartis vaccine for MenB (Bexsero<sup>®</sup>), NHBA stimulates the production of antibodies able to confer protection in humans and covering a wide spectrum of MenB strains (Serruto *et al.*, 2012). NHBA is a surface-exposed lipoprotein, expressed also by non-B serogroups, characterized by an arginine-rich domain responsible for the binding to heparin and heparan sulphate (Serruto *et al.*, 2010). This binding ability is a feature shared by several bacterial virulence factors and

vaccine components (Chen *et al.*, 1995, Menozzi *et al.*, 1996, de Vries *et al.*, 1998). Heparin binding improves the survival of the bacterium in the human serum, while the binding to heparan sulphate has been often related to the pathogen capacity of adhering and invading the host cells; accordingly, heparan sulphate occurs as a proteoglycan on the surface of many cell types, where it plays a role in several aspects of the cell biology (Iozzo, 1998, Gallagher, 2000).

NHBA can be cleaved upstream or downstream of the arginine-rich region by bacterial or host proteases. When NHBA is cleaved by the surface-exposed *Neisseria* peptidase NalP, it generates a fragment called C2 that maintains the arginine-rich domain; alternatively, NHBA can be cleaved by human lactoferrin (hLf), generating the fragment named C1, in which the arginine-rich domain is absent (Fig. S1). Both fragments are released from the bacteria into the culture medium (Serruto *et al.*, 2010). Since the C2 fragment conserves the domain responsible for the binding to heparin, it is plausible that this fragment might interact with secreted or cell-associated proteoglycans in order to exert its own biological role. If this were the case, hLf would have a protective role for the host by generating a fragment (C1) which lacks the active binding domain (Serruto *et al.*, 2010).

It is currently the subject of speculation whether the two fragments possess a specific activity and whether they exert a role in the pathogenesis of *N. meningitidis*-associated disease.

It has been recently reported that interaction of *N. meningitidis* with the host endothelium, mediated by type IV pili, leads to a destabilization of endothelial junctions, thus facilitating the leakage of bacteria from the vessel lumen and the invasion of the central nervous system (Coureuil *et al.*, 2009, Coureuil *et al.*, 2010). However, stable adhesion of bacteria to endothelia could enable other bacterial factors, maybe locally released and therefore reaching great concentrations, to contribute in altering the endothelial barrier. This is expected to occur more likely in case of sepsis, a condition associated with the highest level of bacteraemia (Ovstebo *et al.*, 2004).

1  
2  
3  
4  
5  
6  
7  
8  
9  
10  
11  
12  
13  
14  
15  
16  
17  
18  
19  
20  
21  
22  
23  
24  
25  
26  
27  
28  
29  
30  
31  
32  
33  
34  
35  
36  
37  
38  
39  
40  
41  
42  
43  
44  
45  
46  
47  
48  
49  
50  
51  
52  
53  
54  
55  
56  
57  
58  
59  
60

The aim of the present study was to evaluate whether NHBA-derived fragments may affect endothelial integrity. We demonstrated that C2, but not C1, increases endothelial permeability with a mechanism involving the production of oxygen radicals and the phosphorylation and degradation of the adherens-junction protein VE-cadherin. Collectively, our data suggest that the C2 fragment may be one of the bacterial factors involved in the vascular leakage typical of *purpura fulminans*.

For Peer Review

## Results

### The C2 fragment increases microvasculature endothelial permeability

Our first aim was to verify whether the two fragments, C1 and C2, produced upon cleavage of the full-length NHBA, are involved in the alteration of endothelial permeability. To this end, we used confluent HBMEC monolayers cultured in Transwell cell culture chambers. Permeability leakage of BSA-FITC through the cellular monolayer was measured upon the apical administration of 5  $\mu$ M NHBA, C1, C2 or 1  $\mu$ M bradykinin (BK), as positive control. As shown in Fig. 1A, similarly to BK, the C2 fragment increased endothelial permeability already after 15 min, an effect that became stronger after 30 min and even more after 45 min. Notably, neither the C1 fragment nor the full-length protein NHBA were able to produce a similar effect. Moreover, the alteration of the monolayer integrity, which was not due to a toxic effect (Fig. S2), occurred only if the C2 fragment was administrated to the apical side of endothelia, whereas nothing occurred if the exposure was carried out on the baso-lateral side (data not shown). A dose-response carried out with C2, revealed that at 45 min the peptide was capable of altering endothelial permeability already at 500 nM (Fig. 1B), while at 30 min the leakage became statistically significant at 1  $\mu$ M (data not shown). Considering that 5  $\mu$ M was the lowest concentration at which C2 perturbed the endothelium already after 15 min, we decided to adopt this dose for further experiments. When the transendothelial permeability assay was performed in the presence of antibodies raised against the full-length protein (NHBA), against C2 or just against the arginine-rich domain, the C2 effect was strongly prevented. Notably, no inhibition was observed in the presence of isotypic antibodies, raised against an unrelated antigen (Fig. 1C). The inhibition was also observed in the presence of antibodies anti-NHBA-GNA1030, the fusion protein included in the Bexsero<sup>®</sup> MenB vaccine (Donnelly *et al.*, 2010).

1  
2  
3  
4  
5  
6  
7  
8  
9  
10  
11  
12  
13  
14  
15  
16  
17  
18  
19  
20  
21  
22  
23  
24  
25  
26  
27  
28  
29  
30  
31  
32  
33  
34  
35  
36  
37  
38  
39  
40  
41  
42  
43  
44  
45  
46  
47  
48  
49  
50  
51  
52  
53  
54  
55  
56  
57  
58  
59  
60

**C2 localizes within mitochondria**

In order to address how C2 elicited endothelial perturbation, we investigated its sub-cellular localization within host endothelial cells. First, we took advantage of software capable of predicting a possible localization of a peptide within cells. Among these, we used the MitoProt package (<http://ihg.gsf.de/ihg/mitoprot.html>), which defines whether an N-terminal protein region contains a mitochondrial targeting sequence. The software attributes a score value ranging from 1 to 0, depending on whether the sequence analyzed is more or less compatible with mitochondrial localization. In case of C2, MitoProt yielded a score of 0.7152, which strongly suggested a mitochondrial localization. Indeed, the N-terminal domain of C2 is enriched in basic residues (arginines), that usually confer to a protein the ability of targeting mitochondria (von Heijne, 1986). On the contrary, for NHBA and C1, MitoProt yielded a score of 0.205 and 0.0199, respectively. In order to verify whether the bioinformatics prediction was accurate, we incubated HBMECs with C2, before proceeding with the isolation of mitochondrial, microsomal and cytosolic fractions, at different time points. The protein content of all the fractions was analyzed by western blot for evaluating the presence of C2 and possibly defining its intracellular trafficking. Fig. 2A shows that, after 5 min, C2 was detectable both in microsomes and in the cytosol, while, 15 min after its administration, a fraction of C2 accumulated in mitochondria. After 45 min, C2 was entirely confined to the latter organelle. Independently of the sub-cellular localization, C2 always maintained the N-terminal domain, as demonstrated by the fact that the antibodies anti-arginine-rich peptide revealed the protein. Immunofluorescence analysis performed on cells exposed to C2 allowed us to exclude that the peptide localization within mitochondria was due to a co-segregation of C2 with mitochondrial fraction occurring post lysis (Fig. S3).

In order to confirm the specific localization of the C2 fragment within mitochondria, the same sub-cellular fractionation and analysis was carried on HBMECs exposed to C1; as expected, the peptide did not show any accumulation in mitochondria and, additionally, it was undetectable in the other two



fractions (Fig. 2A). We excluded that C1 was not detected because of the inability of the antibodies to recognize it: indeed, a western blot performed on recombinant C1, revealed that the latter was recognized similarly to C2 by antibodies against the full-length protein NHBA. (Fig. 2B). This result confirms the crucial role of the arginine domain of C2 for its biological activity and indicates that C1 has poor propensity to interact with the cells (Fig. S3).

## C2 induces mitochondrial ROS production

The integrity of endothelial barrier can be perturbed by ROS. For instance, it is well documented that VEGF induces ROS production and alters the monolayer integrity of the endothelial tissue. Although the relationship between ROS and endothelial permeability is not fully understood, it is known that the production of intracellular ROS leads to the phosphorylation of VE-cadherin and  $\beta$ -catenin (both proteins of the adherens junctions) (Monaghan-Benson *et al.*, 2009).

The mitochondrial electron transport chain is one of the major cellular generators of reactive oxygen species, which include superoxide, hydrogen peroxide and the hydroxyl free radical (Loschen *et al.*, 1971, Boveris *et al.*, 1972, Chance *et al.*, 1979). Following the observation that C2 localizes in mitochondria, we decided to verify whether the increased endothelial permeability, caused by the fragment, could follow ROS production within the organelle. Microscopic imaging applied to HBMECs, loaded with the fluoroprobe MitoSOX Red, that permits quantitative detection of mitochondrial superoxide production (Mukhopadhyay *et al.*, 2007), showed significant increase in mitochondrial fluorescence intensity in the cells following the administration of C2, but not of C1 (Fig. 3A). As expected, pre-treatment of the cells with the ROS scavenger N-acetylcysteine (NAC) fully prevented the C2-induced fluorescence increase (Fig. 3A).

Mitochondrial  $H_2O_2$  generation in confluent HBMECs was also evaluated in cells overexpressing mitochondria-targeted HyPer-dMito, which is a fully genetically encoded fluorescent sensor capable of

1  
2  
3  
4  
5  
6  
7  
8  
9  
10  
11  
12  
13  
14  
15  
16  
17  
18  
19  
20  
21  
22  
23  
24  
25  
26  
27  
28  
29  
30  
31  
32  
33  
34  
35  
36  
37  
38  
39  
40  
41  
42  
43  
44  
45  
46  
47  
48  
49  
50  
51  
52  
53  
54  
55  
56  
57  
58  
59  
60

detecting mitochondrial H<sub>2</sub>O<sub>2</sub> in a highly specific manner (Belousov *et al.*, 2006). The probe has two excitation peaks at 420 nm and 500 nm and one emission peak at 516 nm. Upon ROS induction, the excitation peak at 420 nm decreases proportionally to the increase of the peak at 500 nm, allowing ratiometric measurements.

As shown in Fig. 3B, the exposure of cells to the C2 fragment was characterized by a fluorescence ratio decrease while, on the contrary, it remained constant following C1 administration as well as in control cells. ROS increase was appreciable in few minutes with both methods, although with different kinetics: this reflects the nature of the probes, MitoSOX and HyPer-dMito, that are irreversibly and reversibly oxidized, respectively (Lukyanov *et al.*, 2013).

In accordance with the previous experiment, the scavenging of H<sub>2</sub>O<sub>2</sub> by NAC prevented fluorescence ratio decrease (Fig. 3B).

**Reactive oxygen species are required for C2-induced endothelial permeability alteration**

Next, we wondered whether ROS production induced by C2 was involved in the alteration of the endothelial integrity; in order to address this possibility, we repeated the permeability assays on HBMECs, seeded on Transwell, in the presence or absence of NAC.

The results shown in Fig. 4 reveal that, at any considered time point, the ROS scavenger NAC significantly reduced the passage of BSA-FITC through the monolayer: the accumulation of the marker in the lower chamber of the apparatus was similar to that measured following the application of C1, which, as expected, was insensitive to the presence of the scavenger.

Collectively, these data support the conclusion that perturbation of endothelial cells, due to C2, requires intracellular accumulation of ROS; the latter being mainly produced within mitochondria where C2 localizes.

## C2 induces VE-cadherin phosphorylation in a ROS-dependent manner

It has been reported that VEGF leads to the generation of ROS, which, in turn, elevates the tyrosine phosphorylation of VE-cadherin, ultimately regulating adherens junction integrity (Monaghan-Benson *et al.*, 2009, Lee *et al.*, 2011). VE-cadherin phosphorylation, induced by VEGF and by other mediators, such as histamine and bradykinin, is followed by the internalization and ubiquitination of the junctional protein, leading to the opening of endothelial cells junctions (Andriopoulou *et al.*, 1999, Orsenigo *et al.*, 2012).

We sought to determine if the C2-induced increase in microvascular permeability could be associated with the tyrosine phosphorylation of VE-cadherin. For this purpose, we used endothelial cells derived from murine embryonic stem cells with homozygous null mutation of the VE-cadherin gene and overexpressing wild-type human VE-cadherin (Zanetti *et al.*, 2002). We decided to take advantage of this cell model because of the high expression of the junctional protein with respect to HBMECs. In order to abolish the basal phosphorylation rate that commonly occurs in cells (Vincent *et al.*, 2004), the endothelial monolayer was serum-starved for 24 h before being exposed to C2. After VE-cadherin immunoprecipitation, the phosphorylation state of the protein tyrosines was evaluated by western blot. Fig. 5A shows that, already after 5 min of treatment, VE-cadherin was phosphorylated in cells exposed to the C2 fragment, and the phosphorylation level increased further up to 15 min, before decreasing at 45 min. As expected, when cells overexpressing the junctional protein were pre-treated with NAC, the fragment was no longer able to cause phosphorylation of VE-cadherin (Fig. 5B), suggesting that ROS are required for the phosphorylation of the protein. Notably, pre-treatment of cells with the Src kinase inhibitor SU6656 also fully prevented the phosphorylation of VE-cadherin (Fig. 5B), as already reported for VEGF (Weis *et al.*, 2005). Finally, incubation with anti-C2 antibodies also impaired the effect elicited by C2 (Fig. 5B).

1  
2  
3  
4  
5  
6  
7  
8  
9  
10  
11  
12  
13  
14  
15  
16  
17  
18  
19  
20  
21  
22  
23  
24  
25  
26  
27  
28  
29  
30  
31  
32  
33  
34  
35  
36  
37  
38  
39  
40  
41  
42  
43  
44  
45  
46  
47  
48  
49  
50  
51  
52  
53  
54  
55  
56  
57  
58  
59  
60

**C2 promotes VE-cadherin endocytosis**

Phosphorylation of VE-cadherin is associated with the internalization of the junctional protein via the endo-lysosomal pathway (Xiao *et al.*, 2003). Therefore, based on the phosphorylation of VE-cadherin upon the exposure of the cells to C2, we investigated the localization of the junctional protein in the same cells in response to the fragment. We took advantage of a monoclonal antibody (BV6) which recognizes the extracellular domain of VE-cadherin (Gavard *et al.*, 2006). Murine cells overexpressing VE-cadherin were incubated with the antibody at 4°C, to block cellular trafficking, then exposed to C2 for 45 min at 37°C. We chose this time point with the aim to correlate the localization of VE-cadherin with the maximal effect of C2 on the endothelial monolayer integrity. VE-cadherin internalization was monitored by revealing the protein-antibody complex, by applying a secondary antibody in permeabilized cells. Figure 6 shows that C2 stimulation led to the intracellular accumulation of VE-cadherin which acquired a vesicular distribution. In contrast, few sparse vesicles were observed in cells exposed to saline (control). Interestingly, if cells were exposed to C2 in the presence of NAC, the VE-cadherin pattern was similar to that of control, as expected. The absence of any cell-surface staining, independently of the treatment, was due to a mild acid wash, which removed the amount of antibody bound to the membrane-associated VE-cadherin: this approach permitted to better distinguish cell surface cadherin from the internalized one.

**C2 decreases VE-cadherin intracellular content**

The observation that VE-cadherin was internalized raised the possibility that it might be also degraded. Therefore, we quantified the total VE-cadherin content in cells exposed to C2 by a cell-based ELISA and by flow cytometry analysis. With the aim of recapitulating and reinforcing the evidence obtained with the murine cells overexpressing VE-cadherin, we returned to the original cell model, feeling confident in the high sensitivity of the two technical approaches. As shown in Figure 7, the exposure of

1  
2  
3 post-confluent HBMECs to C2 for 45 min reduced by about 20% the VE-cadherin content which  
4  
5 remained low even if the treatment was extended to 3 h. Notably, NAC pre-treatment almost fully  
6  
7 prevented the C2-induced VE-cadherin disappearance (Fig. 7A and D). The same effect was observed  
8  
9 in cells exposed to C2 in the presence of anti-C2 antibodies (Fig. 7B and E).

10  
11 Consistent with the fact that C2 induced phosphorylation of VE-cadherin and that the latter was  
12  
13 abolished when Src kinase was inhibited, the blockage of Src by SU6656, before the administration of  
14  
15 C2, significantly counteracted VE-cadherin reduction (Fig. 7B and E). Finally, the blockage of the  
16  
17 fusion between endosomes and lysosomes by chloroquine, maintained the total cell content of VE-  
18  
19 cadherin similar to that of control cells.

20  
21 Collectively, our data suggest that C2 leads to the generation of ROS, which, in turn, elevate the  
22  
23 tyrosine phosphorylation of the junctional protein VE-cadherin. The latter event, probably mediated at  
24  
25 least in part by Src kinase, is followed by the endocytosis and subsequent degradation of the protein.  
26  
27 The removal of VE-cadherin from the junctional complex is expected to be responsible for the  
28  
29 increased permeability of the endothelial monolayers upon exposure to C2.  
30  
31  
32  
33  
34  
35  
36  
37  
38  
39  
40  
41  
42  
43  
44  
45  
46  
47  
48  
49  
50  
51  
52  
53  
54  
55  
56  
57  
58  
59  
60

1  
2  
3  
4  
5  
6  
7  
8  
9  
10  
11  
12  
13  
14  
15  
16  
17  
18  
19  
20  
21  
22  
23  
24  
25  
26  
27  
28  
29  
30  
31  
32  
33  
34  
35  
36  
37  
38  
39  
40  
41  
42  
43  
44  
45  
46  
47  
48  
49  
50  
51  
52  
53  
54  
55  
56  
57  
58  
59  
60

**Discussion**

In this study, we demonstrate that a fragment originating from the cleavage of the Neisserial Heparin Binding Antigen (NHBA), by the bacterial protease NalP and referred to as C2, increases the permeability of endothelial monolayers. Once applied to the apical side of endothelial cells, C2 quickly accumulates in mitochondria where it stimulates the production of oxygen radicals. The specific targeting of C2 resides in its N-terminal arginine-rich domain; indeed, C1, another NHBA-derived fragment resulting from the proteolysis by the human lactoferrin (Serruto *et al.*, 2010) and differing from C2 because it lacks the arginine sequence, does not localize to mitochondria. Our evidence is in accordance with observations made by other authors testifying that arginines improve membrane permeability and mitochondrial accumulation of proteins (Mitchell *et al.*, 2000, Borgese *et al.*, 2001, Zanetti *et al.*, 2002, Nakase *et al.*, 2012). However, the fact that in heparinase-treated HBMEC monolayers the leakage due to C2 was almost completely compromised (data not shown), suggest that proteoglycans are essential at least for the docking of the protein to the plasma membrane.

C1 does not reach mitochondria, it is unable to trigger ROS production, and does not alter endothelial permeability. Therefore, it is plausible that the ability of C2 in affecting the endothelial barrier is related to its subcellular localization and to the accumulation of ROS. Moreover, C2 has to be applied on the apical side of the endothelial monolayer to alter its integrity and this suggests that *in vivo* it could work within the microvasculature when bacteria form microcolonies along the vascular wall or aggregates inside the lumen of blood vessels (Coureuil *et al.*, 2009, Dupin *et al.*, 2012).

The role of ROS in C2-induced perturbation of endothelial permeability became clear when we found that the administration of the fragment to mouse embryonic cells overexpressing VE-cadherin resulted in an increased tyrosine phosphorylation of the protein, which is a major component of the adherens junctions, and that this event was prevented by NAC. These data suggested that C2 could activate a Src kinase by means of ROS; accordingly, it is established that these enzymes are redox-

regulated proteins (Giannoni *et al.*, 2010). The fact that, when C2 was administrated to cells previously exposed to a Src inhibitor, VE-cadherin phosphorylation was impaired, definitely strengthened the idea that C2 activates Src and that this is achieved by acting through redox signalling.

We found that C2 decreases by about 20% the VE-cadherin content in HBMECs and this effect is almost fully prevented by both NAC and Src inhibitor. Moreover, we demonstrated that the reduction of the junctional protein relies on its enhanced internalization via the endo-lysosomal pathway, a physiological process culminating in the degradation of VE-cadherin that controls the adhesive properties of the cells (Xiao *et al.*, 2003).

It is established that *N. meningitidis*, having left the upper respiratory tract, reaches the bloodstream where it interacts and modifies the properties of the endothelium by triggering intracellular signalling: this occurs in case of meningitis as well as in case of sepsis-associated *purpura fulminans* and results in an increased paracellular permeability (Coureuil *et al.*, 2013). In both situations it has been demonstrated that the main role is exerted by the type IV pili, at least for the Meningococcus strain C, and the molecular mechanism that involves these structures in perturbing the endothelium is well defined mainly in case of brain microvasculature. Type IV pili initially permit the adhesion of bacteria to the endothelium and subsequently, via a  $\beta$ -adrenoreceptor/ $\beta$ -arrestin pathway, lead to the recruitment of junctional proteins under bacterial colonies, weakening the endothelial barrier and thus permitting the passage of bacteria. The activation of  $\beta$ -arrestin leads also to the recruitment and activation of the kinase Src which is involved in the formation of actin-rich cellular protrusions (Coureuil *et al.*, 2009, Coureuil *et al.*, 2010).

With the present study, we demonstrated that the fragment C2 perturbs endothelial integrity through a Src-dependent pathway. Notably, it was shown that pili expression is downregulated during prolonged infection experiment, once bacteria microcolonies are formed (Morand *et al.*, 2004), therefore it is

1  
2  
3  
4  
5  
6  
7  
8  
9  
10  
11  
12  
13  
14  
15  
16  
17  
18  
19  
20  
21  
22  
23  
24  
25  
26  
27  
28  
29  
30  
31  
32  
33  
34  
35  
36  
37  
38  
39  
40  
41  
42  
43  
44  
45  
46  
47  
48  
49  
50  
51  
52  
53  
54  
55  
56  
57  
58  
59  
60

plausible that a second mechanism, maybe involving C2, contribute to the activity of pili in perturbing the endothelial barrier.

In conclusion, with this study we demonstrate that the NHBA-derived fragment C2 alters endothelial permeability causing vascular leakage, a clinical feature particularly evident in the case of meningococemia with high bacteremia and purpuric lesions (Coureuil *et al.*, 2013). The recent setting up of an animal model for meningococcal infection, in which human skin is xenografted into SCID/beige mice (Melican *et al.*, 2013), would be useful for confirming the impact of NHBA-derived C2 during the meningococcus-related diseases.



## Experimental Procedures

### *Reagents*

Phosphate-buffered saline (PBS), D-MEM High Glucose and Foetal bovine serum (FBS) were purchased from Euroclone. Gentamicin and Hepes were purchased from Gibco. Endothelial cells growth supplement (ECGS), BSA-FITC, Red Ponceau, tetramethylbenzidine (TMB) and TMB Stop Solution (1 M sulphuric acid), MEM non essential aminoacids, MEM vitamins, BSA, type-B gelatine, N-acetylcysteine (NAC), DTT, mouse control serum and Tween-20 were obtained from Sigma-Aldrich. Nitrocellulose membrane, 5-ml His Trap HPcolumn, X-ray film and ECL (enhanced chemiluminescence system) were purchased from GE Healthcare. BCA protein assay reagent was purchased from Pierce. Mitosox Red, Alexa Fluor 488-conjugated anti mouse secondary antibody and Alexa Fluor 594-conjugated anti rabbit secondary antibody, 4-12% and 10% SDS-PAGE gels, LDS 4X sample buffer, NuPAGE antioxidant, NuPAGE MES 20X Running Buffer, NuPAGE 20x Transfer Buffer were obtained from Invitrogen. VEGF was obtained from Immunological Sciences. Mitochondria Isolation kit and QiAMP mini-prep Kit were purchased from Qiagen. SU6656, monoclonal anti-GAPDH antibody and monoclonal anti-Ve-cadherin (BV6) were purchased from Merck-Millipore. Rabbit polyclonal anti-TOM20, goat polyclonal antibody labelled with phycoerythrin (PE) anti VE-cadherin, goat polyclonal and monoclonal anti-VE-cadherin antibodies and agarose-coupled Protein G and A were from Santa Cruz Biotechnology. Rabbit polyclonal antibody against EEA1 was from Abcam and monoclonal antibody against phosphotyrosine (clone G410) was obtained from Upstate Biotechnolgy. Monoclonal antibody anti-respiratory chain complex II (COX II) was purchased from Mitosciences. 8-well chambers slide and NU-serum IV were obtained from BD Biosciences. Annexin-V conjugated to Alexa 488 was purchased from Bender MedSystem.

1  
2  
3  
4  
5  
6  
7  
8  
9  
10  
11  
12  
13  
14  
15  
16  
17  
18  
19  
20  
21  
22  
23  
24  
25  
26  
27  
28  
29  
30  
31  
32  
33  
34  
35  
36  
37  
38  
39  
40  
41  
42  
43  
44  
45  
46  
47  
48  
49  
50  
51  
52  
53  
54  
55  
56  
57  
58  
59  
60

*Cell culture*

Simian virus 40 large T antigen-transformed human brain microvascular endothelial cells (HBMEC) were kindly provided by Novartis Vaccines and Diagnostics s.r.l. (Siena, Italy) and were cultured in T75 flasks, in FBS/NU-serum IV-supplemented DMEM high glucose plus non-essential aminoacids and vitamins, to a confluent monolayer. For *in vitro* permeability assays, cells were split and seeded on gelatine-coated Transwell cell culture chambers (polycarbonate filters, 0.3 µm or 3 µm pore size; Corning Costar Corporation, Cambridge, MA, USA) at a density of  $7 \times 10^4$  cells per well. Cells were grown for 5 days before performing permeability assays.

Endothelial cells derived from murine embryonic stem cells with homozygous null mutation of the VE-cadherin gene and overexpressing wild-type human VE-cadherin (Lampugnani *et al.*, 2002, Grazia Lampugnani *et al.*, 2003) were kindly provided by E. Dejana (IFOM, Milan, Italy). Cells were maintained in culture in T75 flasks in FBS-supplemented DMEM high glucose plus heparin and ECGS.

*Preparation of antisera and IgG purification*

Preparation of anti-NHBA, anti-NHBA-GNA1030, anti-C1 and anti-C2 sera is described elsewhere (Serruto *et al.*, 2010). The peptide CSFARFRRSARSRR, corresponding to the arginine-rich domain at the N-terminus of C2 plus a terminal cysteine, was conjugated to Keyhole Limpet Hemocyanin (KLH) using an Inject Activated Immunogen Conjugation Kit (Pierce) and injected into rabbits. The anti-peptide antibodies generated (referred to as anti-Arg-seq) were purified by affinity chromatography on SulfoLink coupling gels (Pierce) onto which the peptide was conjugated. Animal protocols were approved by the local animal ethical committee and by the Italian Minister of Health in accordance with Italian law.

Polyclonal IgG were purified from mouse control serum and from antisera using a mix of Sepharose A and G beads. Briefly, sera were diluted to 1 ml in binding buffer (1.5 M Glycine/NaOH, pH 9.0, 3 M

NaCl), added to the Sepharose beads mix and incubated overnight on an end-over shaker at 4°C. IgG were eluted in 150 µl of elution buffer (0.2 M Glycine/HCl buffer pH 2.5) and neutralized with neutralization buffer (1 M Tris/HCl, pH 9.0). A final concentration of 250 µg/ml of isolated IgG was used in the permeability assays, considering a concentration of specific antibodies of about 10% of total IgG (25 µg/ml).

### *Construction of plasmids and protein expression*

For the expression of all the recombinant proteins considered in this study, the specific DNA fragments were amplified by PCR from *N. meningitidis* MC58 genomic DNA and cloned into the pET-21b+ expression vector (Invitrogen), as detailed elsewhere (Serruto *et al.*, 2010). Purification of recombinant NHBA and of recombinant fragments C1 and C2 have also been previously reported (Serruto *et al.*, 2010). SE-UPLC (size exclusion chromatography) and RP-HPLC (reverse phase chromatography) applied to the purified peptides revealed a purity of greater than or equal to 93%.

### *Permeability assays*

HBMECs were seeded onto 2% gelatine-coated Transwell filters (0.3 µm pore size) at the density of  $7 \times 10^4$  cells per well in a 24-well plate. Cells were used 5 days after seeding onto filters. The formation of intact monolayer on the insert was evaluated by adding FITC-BSA (1 mg/ml) to the upper chamber and measuring after 5 min the amount of labelled BSA passed into the lower chamber by a Fluostar microplate reader (SLT Lab Instruments). Transwells were used only when the intensity of fluorescence in the lower chamber was negligible; in this case, the stimuli were added to the upper chamber together with FITC-BSA, and the fluorescence was evaluated in the lower chamber at various time intervals. Calibration curves were set up measuring the fluorescence intensity of increasing concentrations of

1  
2  
3  
4  
5  
6  
7  
8  
9  
10  
11  
12  
13  
14  
15  
16  
17  
18  
19  
20  
21  
22  
23  
24  
25  
26  
27  
28  
29  
30  
31  
32  
33  
34  
35  
36  
37  
38  
39  
40  
41  
42  
43  
44  
45  
46  
47  
48  
49  
50  
51  
52  
53  
54  
55  
56  
57  
58  
59  
60

FITC-BSA. When required, cells were exposed to 1 mM N-acetylcysteine (NAC) 30 min before adding the stimuli. For evaluating the blocking activity of antibodies anti-NHBA, anti-NHBA-GNA1030, anti-C2 and anti-Arg sequence, they were singularly preincubated with C2 (1 h at 37°C) before addition to the endothelial monolayers. Isotypic antibodies were applied as negative control.

*Cell viability assay*

Cells were incubated with the phosphatidylserine-binding protein Annexin-V conjugated to Alexa 488, according to the manufacturer's instructions. Viability was measured by flow cytometry (FACSCalibur, BD Biosciences, San Jose, CA, USA) and expressed as percentage of Annexin-V-negative events in the gated population.

*Mitochondria isolation*

HBMECs were seeded onto T75 flasks and, once confluent, were exposed to 5 µM C1 or C2 for 5, 15 and 45 min. Cells were collected, washed in ice-cold PBS and processed by Qiagen Mitochondria Isolation Kit. Protein content of isolated fractions, corresponding to mitochondria, cytosol and microsomal fraction, was determined by BCA assay. 10 µg of each fraction were loaded on SDS-PAGE 4-12% and analyzed by western blot.

*Immunoprecipitation*

Murine endothelial cells overexpressing wild-type human VE-cadherin were grown in T75 flasks. Cell layers were serum-starved for 1 day before the application of stimuli. 5 µM C2 was added for 5, 15 and 45 min. Anti-C2 antibody was used at the final concentration of 25µg/ml. When required, cells were pre-incubated for 30 min with 1 mM NAC or with 280 nM SU6656. Cells, detached by scraping, were

collected, washed in ice-cold PBS and lysed in 1% (vol/vol) Triton X-100 in 20 mM Tris-HCl, pH 8.0, and 150 mM NaCl (supplemented with 0.2 mg/mL Na orthovanadate, 1 mg/mL pepstatin, leupeptin, and aprotinin and 10 mM PMSF). Post-nuclear supernatants were immunoprecipitated using 2 µg goat polyclonal anti-VE-cadherin coupled to protein G agarose. Immunoprecipitates were resolved by SDS-PAGE. Phosphorylated VE-cadherin was revealed using an anti-phosphotyrosine antibody followed by peroxidase-labeled secondary antibodies according to the manufacturer's instructions. A goat polyclonal antibody anti-total VE cadherin was used as control for equal loading. Western blots were developed by ECL (Thermo, Fisher Scientific).

### *Measurement of changes in mitochondrial ROS production in HBMECs*

HBMECs were grown on 24 mm diameter glass dishes until confluence; the medium was removed and replaced with HBSS buffer plus  $\text{Ca}^{2+}$  and  $\text{Mg}^{2+}$ , 10 mM Glucose and 4 mM Hepes. Cells were incubated for 30 min with 1 mM Mitosox Red, before starting the live imaging recording. Imaging was performed with an inverted microscope (Olympus IX50); fluorescence emission at 560 nm, upon excitation at 514 nm, was recorded; images were acquired every 10 seconds with a 60X, 1.4 NA oil immersion objective (Olympus) using the Cell<sup>R</sup> software. Stimuli added were 5 µM C1 or C2; when required, cells were pre-treated 30 min with 1 mM NAC. Data were expressed as  $F/F_0$ , where  $F$  is the fluorescence emission intensity at time  $t$  and  $F_0$  is the fluorescence emission intensity at time = 0.

Mitochondrial  $\text{H}_2\text{O}_2$  generation in confluent HBMECs was also evaluated in cells transfected with 2 µg of mitochondria-targeted HyPer-Mito (Evrogen, [www.evrogen.com](http://www.evrogen.com)), which is a fully genetically encoded fluorescent sensor capable for highly specific detection of mitochondrial  $\text{H}_2\text{O}_2$  (Belousov *et al.*, 2006). Following the application of stimuli (5 µM C1 or C2), in HBSS buffer plus  $\text{Ca}^{2+}$  and  $\text{Mg}^{2+}$ , 10 mM glucose, 4 mM Hepes, fluorescence emission at 516 nm was recorded (10 s intervals) using an Olympus IX81 microscope following excitation at 420 nm and 500 nm. When required, cells were pre-

1  
2  
3  
4  
5  
6  
7  
8  
9  
10  
11  
12  
13  
14  
15  
16  
17  
18  
19  
20  
21  
22  
23  
24  
25  
26  
27  
28  
29  
30  
31  
32  
33  
34  
35  
36  
37  
38  
39  
40  
41  
42  
43  
44  
45  
46  
47  
48  
49  
50  
51  
52  
53  
54  
55  
56  
57  
58  
59  
60

treated 30 min with 1 mM NAC. The ratio (R) between the emission values at the two wavelengths of excitation (420/500) was calculated. Data were expressed as  $R/R_0$ , where R is the ratio at time t and  $R_0$  is the ratio at time = 0.

*Immunofluorescence*

HBMECs seeded ( $0.5 \times 10^4$ /ml) on 8-well chamber slides (BD Biosciences) were exposed to C1 or C2 for 45 min. Cells were then fixed with 3.7% formaldehyde in PBS for 30 min, permeabilized with 0.01% Nonidet P40 in PBS for 20 min at RT and blocked with PBS 0.5% BSA. TOM20, adopted as mitochondrial marker, was revealed with a rabbit polyclonal antibody followed by an ALEXA 594-conjugated anti-rabbit secondary antibody. C1 or C2 were revealed with polyclonal antibodies purified from sera of C1 or C2-immunized mice, followed by ALEXA 488-conjugated anti-mouse secondary antibodies.

*VE-cadherin internalization assay*

The assay was performed using a procedure adapted from a previous report (Paterson *et al.*, 2003). Murine endothelial cells overexpressing wild-type human VE-cadherin were seeded on 8-well chamber slides ( $0.5 \times 10^4$ /ml). Cells were exposed for 1 h at 4°C to a monoclonal antibody directed against the VE-cadherin extracellular domain (BV6), diluted in DMEM 20 mM Hepes, 3% BSA. When required, 1 mM NAC was added 30 min before removing the antibody. Unbound antibody was washed-out by rinsing cells in ice-cold DMEM 20 mM Hepes, 3% BSA. Cells were incubated with 5  $\mu$ M C2 for 45 min at 37 °C in the same medium; where required, NAC was renewed. Cells exposed to saline  $\pm$  NAC were used as controls. To remove cell surface bound antibody, while retaining internalized antibody, cells were washed for 15 min in PBS, pH 2.7 containing 25 mM glycine and 3% BSA. Cells were fixed

with 3.7% formaldehyde in PBS for 30 min, permeabilized with 0.01% Triton X-100 0.5% in PBS for 15 min at RT. The internalized VE-cadherin, complexed with the antibody, was revealed with an ALEXA 488-conjugated anti-mouse secondary antibody, while nuclei were revealed with DAPI. Cells were visualized with a 63X oil immersion objective on a laser-scanning confocal microscope and images were acquired using the LAS-AF software (Leica TCS-SP5, Leica Microsystems, Wetzlar, Germany). Images were then processed using ImageJ (Research Services Branch, National Institute of Mental Health, Bethesda, MD, USA).

#### *Cell-based ELISA for evaluation of VE-cadherin content*

Cell-based ELISA was performed as previously reported (Shen *et al.*, 2011) with minor modifications. Briefly, HBMECs were seeded ( $5 \times 10^4$ /well) onto 96-well plates. Three days after reaching confluence and forming a contact-inhibited monolayer, cells were treated with 5  $\mu$ M C2 for 45 min or 3 h. When required, cells were pre-treated for 30 min with 1 mM NAC, 280 nM SU6656 or 100  $\mu$ M chloroquine for 2 h. For evaluating the effect of anti-C2 antibodies, the latter were added together with C2 at a final concentration of 250  $\mu$ g/ml. Cells were fixed with 3.7% formaldehyde for 10 min at RT and incubated with blocking buffer (PBS with 10% FBS) for 60 min at 37°C. After washing with 0.1% Triton X-100 in PBS, cells were incubated with a goat polyclonal antibody against VE-cadherin (1:500) overnight at 4°C. After washing with PBS, a secondary HRP-conjugated antibody was added and incubated for 1 h at RT. After washing again, TMB solution was added, incubated for 15 min followed by the stop solution for 5 min. The optical density of each well was read at 450 nm using a plate reader (Tecan, Infinite 200 pro, Salzburg, Austria). Results were expressed as percentage of the control group (cells exposed to saline).

1  
2  
3  
4  
5  
6  
7  
8  
9  
10  
11  
12  
13  
14  
15  
16  
17  
18  
19  
20  
21  
22  
23  
24  
25  
26  
27  
28  
29  
30  
31  
32  
33  
34  
35  
36  
37  
38  
39  
40  
41  
42  
43  
44  
45  
46  
47  
48  
49  
50  
51  
52  
53  
54  
55  
56  
57  
58  
59  
60

*Flow cytometry for evaluation of VE-cadherin content*

HBMECs were seeded ( $2 \times 10^5$ /well) in 24-well plates. Three days after reaching confluence and forming a contact-inhibited monolayer, cells were treated with 5  $\mu$ M C2 for 45 min or 3 h. When required, cells were pre-treated with NAC, SU6656 or chloroquine as detailed above. 250  $\mu$ g/ml anti-C2 antibodies were added to the cells together with C2.

Cells were detached with 2 mM Na-EDTA and collected in flow cytometry tube. After washing in PBS, cells were pelleted at 1200 rpm for 5 min at 4°C and fixed and permeabilized with ice-cold methanol in ice for 30 min. A PE-conjugated anti-VE-cadherin antibody was used to label the cytosolic portion of the protein. Cells were analyzed by flow cytometry (FACSCalibur) and data analysis was carried out using CellQuest software (BD Biosciences).

*Statistical analyses*

Statistical significance was calculated by unpaired Student's *t*-test. Data, reported as the mean  $\pm$  S.D., were considered significant if  $p$ -values  $\leq 0.05$ .



## Acknowledgements

We thank L. Santini and F. Ferlicca (Novartis Vaccines and Diagnostics) for providing all the sera, E. Martinelli, M. Giuliani, E. Cartocci and E. Grassi (Novartis Vaccines and Diagnostics) for preparation and purification of recombinant C2 protein and V. Massignani (Novartis Vaccines and Diagnostics) and C. Giampietro (IFOM-IEO Campus) for helpful discussion and advices. This work was partially supported by Italian Ministry of University and Research, Prin projects and Fondazione Cariplo, grant N° 2011-0485 (to MdB).

The authors declare that no conflict of interest exists.

1  
2  
3  
4  
5  
6  
7  
8  
9  
10  
11  
12  
13  
14  
15  
16  
17  
18  
19  
20  
21  
22  
23  
24  
25  
26  
27  
28  
29  
30  
31  
32  
33  
34  
35  
36  
37  
38  
39  
40  
41  
42  
43  
44  
45  
46  
47  
48  
49  
50  
51  
52  
53  
54  
55  
56  
57  
58  
59  
60

References

Andriopoulou, P., Navarro, P., Zanetti, A., Lampugnani, M.G. and Dejana, E. (1999). Histamine induces tyrosine phosphorylation of endothelial cell-to-cell adherens junctions. *Arteriosclerosis, thrombosis, and vascular biology* **19**, 2286-2297.

Belousov, V.V., Fradkov, A.F., Lukyanov, K.A., Staroverov, D.B., Shakhbazov, K.S., Terskikh, A.V. and Lukyanov, S. (2006). Genetically encoded fluorescent indicator for intracellular hydrogen peroxide. *Nature methods* **3**, 281-286.

Borgese, N., Gazzoni, I., Barberi, M., Colombo, S. and Pedrazzini, E. (2001). Targeting of a tail-anchored protein to endoplasmic reticulum and mitochondrial outer membrane by independent but competing pathways. *Molecular biology of the cell* **12**, 2482-2496.

Boveris, A., Oshino, N. and Chance, B. (1972). The cellular production of hydrogen peroxide. *The Biochemical journal* **128**, 617-630.

Caesar, N.M., Myers, K.A. and Fan, X. (2013). Neisseria meningitidis serogroup B vaccine development. *Microb Pathog* **57**, 33-40.

Chance, B., Sies, H. and Boveris, A. (1979). Hydroperoxide metabolism in mammalian organs. *Physiological reviews* **59**, 527-605.

Chen, T., Swanson, J., Wilson, J. and Belland, R.J. (1995). Heparin protects Opa+ Neisseria gonorrhoeae from the bactericidal action of normal human serum. *Infection and immunity* **63**, 1790-1795.

Coureuil, M., Join-Lambert, O., Lecuyer, H., Bourdoulous, S., Marullo, S. and Nassif, X. (2013). Pathogenesis of meningococemia. *Cold Spring Harb Perspect Med* **3**.

Coureuil, M., Lecuyer, H., Scott, M.G., Boularan, C., Enslen, H., Soyer, M., et al. (2010). Meningococcus Hijacks a beta2-adrenoceptor/beta-Arrestin pathway to cross brain microvasculature endothelium. *Cell* **143**, 1149-1160.

Coureuil, M., Mikaty, G., Miller, F., Lecuyer, H., Bernard, C., Bourdoulous, S., et al. (2009). Meningococcal type IV pili recruit the polarity complex to cross the brain endothelium. *Science* **325**, 83-87.

de Vries, F.P., Cole, R., Dankert, J., Frosch, M. and van Putten, J.P. (1998). Neisseria meningitidis producing the Opc adhesin binds epithelial cell proteoglycan receptors. *Molecular microbiology* **27**, 1203-1212.

Donnelly, J., Medini, D., Boccadifuoco, G., Biolchi, A., Ward, J., Frasc, C., et al. (2010). Qualitative and quantitative assessment of meningococcal antigens to evaluate the potential strain coverage of protein-based vaccines. *Proc Natl Acad Sci U S A* **107**, 19490-19495.

Dupin, N., Lecuyer, H., Carlotti, A., Poyart, C., Coureuil, M., Chanal, J., et al. (2012). Chronic meningococemia cutaneous lesions involve meningococcal perivascular invasion through the remodeling of endothelial barriers. *Clin Infect Dis* **54**, 1162-1165.

Gallagher, J.T., and Lyon, M. (2000) Molecular structure of heparan sulfate and interactions with growth factors and morphogens. In *Proteoglycans: structure, biology and molecular interactions.* , R.V. Iozzo (ed.). New York, Marcel Dekker Inc. New York, pp. 27–59.

Gavard, J. and Gutkind, J.S. (2006). VEGF controls endothelial-cell permeability by promoting the beta-arrestin-dependent endocytosis of VE-cadherin. *Nat Cell Biol* **8**, 1223-1234.

Giannoni, E., Taddei, M.L. and Chiarugi, P. (2010). Src redox regulation: again in the front line. *Free radical biology & medicine* **49**, 516-527.

Grazia Lampugnani, M., Zanetti, A., Corada, M., Takahashi, T., Balconi, G., Breviario, F., et al. (2003). Contact inhibition of VEGF-induced proliferation requires vascular endothelial cadherin, beta-catenin, and the phosphatase DEP-1/CD148. *The Journal of cell biology* **161**, 793-804.

Iozzo, R.V. (1998). Matrix proteoglycans: from molecular design to cellular function. *Annual review of biochemistry* **67**, 609-652.

- Lampugnani, M.G., Zanetti, A., Breviario, F., Balconi, G., Orsenigo, F., Corada, M., *et al.* (2002). VE-cadherin regulates endothelial actin activating Rac and increasing membrane association of Tiam. *Molecular biology of the cell* **13**, 1175-1189.
- Lee, M., Choy, W.C. and Abid, M.R. (2011). Direct sensing of endothelial oxidants by vascular endothelial growth factor receptor-2 and c-Src. *PloS one* **6**, e28454.
- Loschen, G., Flohe, L. and Chance, B. (1971). Respiratory chain linked H<sub>2</sub>O<sub>2</sub> production in pigeon heart mitochondria. *FEBS letters* **18**, 261-264.
- Lukyanov, K.A. and Belousov, V.V. (2013). Genetically encoded fluorescent redox sensors. *Biochim Biophys Acta*.
- Melican, K., Michea Veloso, P., Martin, T., Bruneval, P. and Dumenil, G. (2013). Adhesion of *Neisseria meningitidis* to dermal vessels leads to local vascular damage and purpura in a humanized mouse model. *PLoS Pathog* **9**, e1003139.
- Menozzi, F.D., Rouse, J.H., Alavi, M., Laude-Sharp, M., Muller, J., Bischoff, R., *et al.* (1996). Identification of a heparin-binding hemagglutinin present in mycobacteria. *The Journal of experimental medicine* **184**, 993-1001.
- Mitchell, D.J., Kim, D.T., Steinman, L., Fathman, C.G. and Rothbard, J.B. (2000). Polyarginine enters cells more efficiently than other polycationic homopolymers. *The journal of peptide research : official journal of the American Peptide Society* **56**, 318-325.
- Monaghan-Benson, E. and BurrIDGE, K. (2009). The regulation of vascular endothelial growth factor-induced microvascular permeability requires Rac and reactive oxygen species. *The Journal of biological chemistry* **284**, 25602-25611.
- Morand, P.C., Bille, E., Morelle, S., Eugene, E., Beretti, J.L., Wolfgang, M., *et al.* (2004). Type IV pilus retraction in pathogenic *Neisseria* is regulated by the PilC proteins. *EMBO J* **23**, 2009-2017.
- Mukhopadhyay, P., Rajesh, M., Hasko, G., Hawkins, B.J., Madesh, M. and Pacher, P. (2007). Simultaneous detection of apoptosis and mitochondrial superoxide production in live cells by flow cytometry and confocal microscopy. *Nature protocols* **2**, 2295-2301.
- Nakase, I., Okumura, S., Katayama, S., Hirose, H., Pujals, S., Yamaguchi, H., *et al.* (2012). Transformation of an antimicrobial peptide into a plasma membrane-permeable, mitochondria-targeted peptide via the substitution of lysine with arginine. *Chem Commun (Camb)* **48**, 11097-11099.
- Orsenigo, F., Giampietro, C., Ferrari, A., Corada, M., Galaup, A., Sigismund, S., *et al.* (2012). Phosphorylation of VE-cadherin is modulated by haemodynamic forces and contributes to the regulation of vascular permeability in vivo. *Nat Commun* **3**, 1208.
- Ovstebo, R., Brandtzaeg, P., Brusletto, B., Haug, K.B., Lande, K., Hoiby, E.A. and Kierulf, P. (2004). Use of robotized DNA isolation and real-time PCR to quantify and identify close correlation between levels of *Neisseria meningitidis* DNA and lipopolysaccharides in plasma and cerebrospinal fluid from patients with systemic meningococcal disease. *J Clin Microbiol* **42**, 2980-2987.
- Paterson, A.D., Parton, R.G., Ferguson, C., Stow, J.L. and Yap, A.S. (2003). Characterization of E-cadherin endocytosis in isolated MCF-7 and chinese hamster ovary cells: the initial fate of unbound E-cadherin. *J Biol Chem* **278**, 21050-21057.
- Pathan, N., Faust, S.N. and Levin, M. (2003). Pathophysiology of meningococcal meningitis and septicaemia. *Arch Dis Child* **88**, 601-607.
- Serruto, D., Bottomley, M.J., Ram, S., Giuliani, M.M. and Rappuoli, R. (2012). The new multicomponent vaccine against meningococcal serogroup B, 4CMenB: immunological, functional and structural characterization of the antigens. *Vaccine* **30 Suppl 2**, B87-97.
- Serruto, D., Spadafina, T., Ciocchi, L., Lewis, L.A., Ram, S., Tontini, M., *et al.* (2010). *Neisseria meningitidis* GNA2132, a heparin-binding protein that induces protective immunity in humans. *Proceedings of the National Academy of Sciences of the United States of America* **107**, 3770-3775.
- Shen, W., Li, S., Chung, S.H., Zhu, L., Stayt, J., Su, T., *et al.* (2011). Tyrosine phosphorylation of VE-cadherin and claudin-5 is associated with TGF-beta1-induced permeability of centrally derived vascular endothelium. *European journal of cell biology* **90**, 323-332.

1  
2  
3  
4  
5  
6  
7  
8  
9  
10  
11  
12  
13  
14  
15  
16  
17  
18  
19  
20  
21  
22  
23  
24  
25  
26  
27  
28  
29  
30  
31  
32  
33  
34  
35  
36  
37  
38  
39  
40  
41  
42  
43  
44  
45  
46  
47  
48  
49  
50  
51  
52  
53  
54  
55  
56  
57  
58  
59  
60

Vincent, P.A., Xiao, K., Buckley, K.M. and Kowalczyk, A.P. (2004). VE-cadherin: adhesion at arm's length. *American journal of physiology. Cell physiology* **286**, C987-997.

von Heijne, G. (1986). Mitochondrial targeting sequences may form amphiphilic helices. *The EMBO journal* **5**, 1335-1342.

Weis, S.M. and Cheresh, D.A. (2005). Pathophysiological consequences of VEGF-induced vascular permeability. *Nature* **437**, 497-504.

Xiao, K., Allison, D.F., Kottke, M.D., Summers, S., Sorescu, G.P., Faundez, V. and Kowalczyk, A.P. (2003). Mechanisms of VE-cadherin processing and degradation in microvascular endothelial cells. *The Journal of biological chemistry* **278**, 19199-19208.

Zanetti, A., Lampugnani, M.G., Balconi, G., Breviario, F., Corada, M., Lanfrancone, L. and Dejana, E. (2002). Vascular endothelial growth factor induces SHC association with vascular endothelial cadherin: a potential feedback mechanism to control vascular endothelial growth factor receptor-2 signaling. *Arteriosclerosis, thrombosis, and vascular biology* **22**, 617-622.

## Figure Legends

**Fig. 1.** The C2 fragment induces the leakage of HBMECs-formed monolayer.

A. Human brain microvascular endothelial cells (HBMECs), grown as monolayer onto the membrane of a Transwell system, were stimulated with 5  $\mu$ M C2, C1, NHBA, or saline (control). 1  $\mu$ M bradikinin (BK) was used as positive control. The passage of FITC-BSA into the lower chamber, at various time intervals, was evaluated.

B. HBMEC monolayers were exposed to the indicated concentrations of C2 for 45 min. Monolayer leakage was evaluated as in A.

C. HBMEC monolayers were exposed to C2 for 45 min in the presence of the indicated antibodies. Monolayer leakage was evaluated as in A. Values are expressed as means  $\pm$  SD of duplicate determinations of four separate experiments. \*,  $p < 0.05$ ; \*\*,  $p < 0.01$ ; \*\*\*,  $p < 0.001$ .

**Fig. 2.** The C2 fragment accumulates in mitochondria.

A. HBMECs, grown to confluence in a T75 flask, were exposed to 5  $\mu$ M C2, C1 or saline (control). After 5, 15 and 45 min mitochondrial (Mt), microsomal (Mf) and cytosolic (C) fractions were isolated and processed for western blot analysis. A mouse polyclonal anti-NHBA antibody was used to reveal both C1 and C2 peptides. The latter was also revealed by a polyclonal antibody specific for the arginine-rich domain. Monoclonal antibodies anti-COXII, anti-EEA1 and anti-GAPDH were used to check the purity of each fraction. HRP-conjugated secondary antibodies were used before developing in chemiluminescence. The molecular weights of the single proteins are in brackets.

B. Control of the ability of anti-NHBA antibody to recognize the C1 peptide. 0.5  $\mu$ g of C1 and C2 were loaded in SDS-PAGE and processed for western blot as in A, using both anti-NHBA and anti-arginine sequence antibodies. The lower band of C2, not recognized by the anti-arginine sequence, is probably a degradation product of the peptide.

1  
2  
3  
4  
5  
6  
7  
8  
9  
10  
11  
12  
13  
14  
15  
16  
17  
18  
19  
20  
21  
22  
23  
24  
25  
26  
27  
28  
29  
30  
31  
32  
33  
34  
35  
36  
37  
38  
39  
40  
41  
42  
43  
44  
45  
46  
47  
48  
49  
50  
51  
52  
53  
54  
55  
56  
57  
58  
59  
60

**Fig. 3.** C2 induces mitochondrial ROS formation in HBMECs.

A. HBMECs, grown as monolayer, were loaded with 1  $\mu$ M MitoSOX Red, just before live-imaging recording. At the indicated time point (arrow head) cells were exposed to 5  $\mu$ M C1, C2, or saline (control).

When required, cells were pre-treated with 1 mM NAC before being exposed to C2. Cells were excited by laser at 514 nm and fluorescence emitted was recorded at 560 nm every 10 s for 30 min. Data are expressed as  $F/F_0$ , where  $F$  is the fluorescence emission intensity at time  $t$  and  $F_0$  is the fluorescence emission intensity at time = 0. Each kinetics trace is the average of the recording for 3 cells and it is representative of 3 independent experiments performed on different cell preparations. The right panel reports the mean  $\Delta F/F_0 \pm$  SD for the 3 experiments, calculated at 30 min (N=3 cells per experiment).

B. HBMECs, grown as monolayer, were transfected with the Hyper-dMito vector. After 24 h of expression, cells were exposed to 5  $\mu$ M C1, C2, or saline (control). When required, cells were pre-treated with 1 mM NAC before being exposed to C2. Fluorescence intensities were recorded every 10 s for 1 h. Normalized fluorescence ratio changes (420/500 nm) were calculated as a measure of  $H_2O_2$  production. Data are expressed as  $R/R_0$ , where  $R$  is the ratio at time  $t$  and  $R_0$  is the ratio at time = 0. Each kinetics trace is the average of the recording for 3 cells and it is representative of 3 independent experiments performed on different cell preparations. The right panel reports the mean  $\Delta R/R_0 \pm$  SD for the 3 experiments, calculated at 30 min (N=3 cells per experiment). \*\*\*,  $p < 0.001$ .

**Fig. 4.** ROS induced by C2 are essential for the alteration of endothelial permeability.

HBMECs, seeded onto the membrane of a Transwell system, were exposed to 5  $\mu$ M C2 or C1 fragment together with FITC-BSA. When required, HBMECs were pre-treated with 1 mM NAC for 30 min. The accumulation of BSA in the lower chamber was performed as detailed in Figure 1. Values are

expressed as mean  $\pm$  SD of duplicate determinations of four separate experiments. \*,  $p < 0.05$ ; \*\*,  $p < 0.01$ .

**Fig. 5. C2 induces VE-cadherin phosphorylation.**

A. Murine endothelial cells overexpressing wild-type human VE-cadherin were grown to confluence before being serum-starved for 24 h and exposed or not to 5  $\mu$ M C2. After 5, 15 and 45 min, cells were harvested and processed for immunoprecipitation with a polyclonal antibody anti-VE-cadherin. Control is represented by cells exposed to saline for 15 min. Phosphorylation state of the protein was determined in western blot by developing with anti-phosphotyrosine antibody. Total VE-cadherin was used as loading control.

B. Cells were pre-treated or not with NAC or with the Src kinase inhibitor SU6656 for 30 min before the administration of C2. C2 was tested either as such or in the presence of anti-C2 antibodies. Control is represented by cells exposed to saline for 45 min.

**Fig. 6. C2 induces VE-cadherin internalization.**

Murine endothelial cells overexpressing wild-type human VE-cadherin were grown to confluence. To evaluate the internalization of the cell surface-associated VE-cadherin, the junctional protein was labelled at 4°C with a monoclonal antibody specific for the extracellular domain. After C2 exposure for 45 min at 37°C, cells were processed for immunofluorescence revealing the protein-antibody complex by an appropriate secondary antibody. Where required, cells were pre-treated with 1 mM NAC for 30 min. Confocal images were acquired using a Leica microscope with a 63 $\times$  oil immersion objective. Images were merged using ImageJ. Bars: 20  $\mu$ m.

1  
2  
3  
4  
5  
6  
7  
8  
9  
10  
11  
12  
13  
14  
15  
16  
17  
18  
19  
20  
21  
22  
23  
24  
25  
26  
27  
28  
29  
30  
31  
32  
33  
34  
35  
36  
37  
38  
39  
40  
41  
42  
43  
44  
45  
46  
47  
48  
49  
50  
51  
52  
53  
54  
55  
56  
57  
58  
59  
60

**Fig. 7. C2 lowers cellular VE-cadherin content.**

HBMECs were grown to confluence before being exposed to 5  $\mu$ M C2. After 45 min and 3 h a cell-based ELISA (panels A, C and E) and flow cytometry analysis (panels B, D and F) were performed for evaluating the total cell content of VE-cadherin. Values are the mean  $\pm$  SD of three separate experiments, with two determinations per experiment. \*,  $p < 0.05$ ; \*\*,  $p < 0.01$ .

A and D. Where specified, cells were pre-treated with 1 mM NAC for 30 min.

B and E. Where specified, cells were pre-treated with 280 nM SU6656 for 30 min.

C and F. Where specified, cells were pre-treated with 100  $\mu$ M chloroquine for 2 h.



# **The C2 fragment from *Neisseria meningitidis* antigen NHBA increases endothelial permeability by destabilizing adherens junctions**

**Running Title:** C2 fragment from NHBA alters endothelial integrity

**Alessandro Casellato<sup>1</sup>, Silvia Rossi Paccani<sup>2</sup>, Riccardo Barrile<sup>2</sup>, Fleur Bossi<sup>3</sup>, Laura Ciocchi<sup>2</sup>, Gaia Codolo<sup>1,4</sup>, Mariagrazia Pizza<sup>2</sup>, Beatrice Aricò<sup>2</sup>, Marina de Bernard<sup>1,4</sup>**

<sup>1</sup>Venetian Institute of Molecular Medicine, Padua, Italy; <sup>2</sup>Novartis Vaccines and Diagnostics, Siena, Italy; <sup>3</sup>Department of Medicine, Surgery and Health Sciences, University of Trieste, Trieste, Italy;

<sup>4</sup>Department of Biology, University of Padua, Padua, Italy

## **Address correspondence to:**

Prof. Marina de Bernard, Venetian Institute of Molecular Medicine, Via Orus 2, 35129 Padova Italy

e-mail address: marina.debernard@unipd.it, Phone: +39.049.7923223, Fax: +39.049.7923250 and Dr.

Beatrice Aricò, Novartis Vaccines and Diagnostics, Siena, Italy, e-mail address:

beatrice.arico@novartis.com, Phone: +39.0577.243239, Fax: +39.0577.539314.

1  
2  
3  
4  
5  
6  
7  
8  
9  
10  
11  
12  
13  
14  
15  
16  
17  
18  
19  
20  
21  
22  
23  
24  
25  
26  
27  
28  
29  
30  
31  
32  
33  
34  
35  
36  
37  
38  
39  
40  
41  
42  
43  
44  
45  
46  
47  
48  
49  
50  
51  
52  
53  
54  
55  
56  
57  
58  
59  
60

**Summary**

*Neisseria meningitidis* is a human pathogen that can cause fatal sepsis and meningitis once it reaches the blood stream and the nervous system. Here we demonstrate that a fragment, released upon proteolysis of the surface-exposed protein Neisserial Heparin Binding Antigen (NHBA), by the bacterial protease NalP, alters the endothelial permeability by inducing the internalization of the adherens junction protein VE-cadherin. We found that C2 rapidly accumulates in mitochondria where it induces the production of reactive oxygen species: the latter are required for the phosphorylation of the junctional protein and for its internalization that, in turn, is responsible for the endothelial leakage. Our data support the notion that the NHBA-derived fragment C2 might contribute to the extensive vascular leakage typically associated with meningococcal sepsis.

## Introduction

*Neisseria meningitidis* is an encapsulated, Gram-negative bacterium that colonizes the nasopharynx of 8-20% of healthy individuals. In a small proportion of infected patients, the bacterium crosses the mucosal barrier and reaches the bloodstream, giving rise to meningitis or fulminant septicaemia. One of the most dramatic features of severe meningococcal sepsis is the occurrence of widespread *purpura fulminans*, in which disseminated intravascular coagulation is associated with massive vascular leakage and multiple organ failure (Pathan *et al.*, 2003).

13 serogroups of *N. meningitidis* have been identified, on the basis of the specific composition of the polysaccharide capsule, and five of them are associated with the disease (Caesar *et al.*, 2013). Although vaccines containing purified polysaccharide antigens are available against four of the five pathogenic serogroups, the capsular polysaccharide of Meningococcus serotype B (MenB) is not suitable for the formulation of human vaccines. Indeed, the MenB strain is characterized by a capsule made of sialic acid, one of the constitutive sugars of the human cellular glycolyx. Therefore, sialic acid represents a poorly immunogenic self-antigen in humans that cannot be used for vaccination, thus rendering the strategy adopted for the other strains not suitable for MenB. Novartis Vaccines in 2000 overcame this obstacle by adopting an innovative strategy called reverse vaccinology. This bio-informatics method, combined with molecular biology and biochemical techniques, led to the discovery of a plethora of new MenB conserved antigens potentially considered as vaccine candidates. Among these antigens, is the Neisserial Heparin Binding Antigen (NHBA, elsewhere called GNA2132). In combination with the other components of the Novartis vaccine for MenB (Bexsero<sup>®</sup>), NHBA stimulates the production of antibodies able to confer protection in humans and covering a wide spectrum of MenB strains (Serruto *et al.*, 2012). NHBA is a surface-exposed lipoprotein, expressed also by non-B serogroups, characterized by an arginine-rich domain responsible for the binding to heparin and heparan sulphate (Serruto *et al.*, 2010). This binding ability is a feature shared by several bacterial virulence factors and

1  
2  
3  
4  
5  
6  
7  
8  
9  
10  
11  
12  
13  
14  
15  
16  
17  
18  
19  
20  
21  
22  
23  
24  
25  
26  
27  
28  
29  
30  
31  
32  
33  
34  
35  
36  
37  
38  
39  
40  
41  
42  
43  
44  
45  
46  
47  
48  
49  
50  
51  
52  
53  
54  
55  
56  
57  
58  
59  
60

vaccine components (Chen *et al.*, 1995, Menozzi *et al.*, 1996, de Vries *et al.*, 1998). Heparin binding improves the survival of the bacterium in the human serum, while the binding to heparan sulphate has been often related to the pathogen capacity of adhering and invading the host cells; accordingly, heparan sulphate occurs as a proteoglycan on the surface of many cell types, where it plays a role in several aspects of the cell biology (Iozzo, 1998, Gallagher, 2000).

NHBA can be cleaved upstream or downstream of the arginine-rich region by bacterial or host proteases. When NHBA is cleaved by the surface-exposed *Neisseria* peptidase NalP, it generates a fragment called C2 that maintains the arginine-rich domain; alternatively, NHBA can be cleaved by human lactoferrin (hLf), generating the fragment named C1, in which the arginine-rich domain is absent (Fig. S1). Both fragments are released from the bacteria into the culture medium (Serruto *et al.*, 2010). Since the C2 fragment conserves the domain responsible for the binding to heparin, it is plausible that this fragment might interact with secreted or cell-associated proteoglycans in order to exert its own biological role. If this were the case, hLf would have a protective role for the host by generating a fragment (C1) which lacks the active binding domain (Serruto *et al.*, 2010).

It is currently the subject of speculation whether the two fragments possess a specific activity and whether they exert a role in the pathogenesis of *N. meningitidis*-associated disease.

It has been recently reported that interaction of *N. meningitidis* with the host endothelium, mediated by type IV pili, leads to a destabilization of endothelial junctions, thus facilitating the leakage of bacteria from the vessel lumen and the invasion of the central nervous system (Coureuil *et al.*, 2009, Coureuil *et al.*, 2010). However, stable adhesion of bacteria to endothelia could enable other bacterial factors, maybe locally released and therefore reaching great concentrations, to contribute in altering the endothelial barrier. This is expected to occur more likely in case of sepsis, a condition associated with the highest level of bacteraemia (Ovstebo *et al.*, 2004).

1  
2  
3 The aim of the present study was to evaluate whether NHBA-derived fragments may affect endothelial  
4 integrity. We demonstrated that C2, but not C1, increases endothelial permeability with a mechanism  
5 involving the production of oxygen radicals and the phosphorylation and degradation of the adherens-  
6 junction protein VE-cadherin. Collectively, our data suggest that the C2 fragment may be one of the  
7 bacterial factors involved in the vascular leakage typical of *purpura fulminans*.  
8  
9  
10  
11  
12  
13  
14  
15  
16  
17  
18  
19  
20  
21  
22  
23  
24  
25  
26  
27  
28  
29  
30  
31  
32  
33  
34  
35  
36  
37  
38  
39  
40  
41  
42  
43  
44  
45  
46  
47  
48  
49  
50  
51  
52  
53  
54  
55  
56  
57  
58  
59  
60

For Peer Review

1  
2  
3  
4  
5  
6  
7  
8  
9  
10  
11  
12  
13  
14  
15  
16  
17  
18  
19  
20  
21  
22  
23  
24  
25  
26  
27  
28  
29  
30  
31  
32  
33  
34  
35  
36  
37  
38  
39  
40  
41  
42  
43  
44  
45  
46  
47  
48  
49  
50  
51  
52  
53  
54  
55  
56  
57  
58  
59  
60

**Results**

**The C2 fragment increases microvasculature endothelial permeability**

Our first aim was to verify whether the two fragments, C1 and C2, produced upon cleavage of the full-length NHBA, are involved in the alteration of endothelial permeability. To this end, we used confluent HBMEC monolayers cultured in Transwell cell culture chambers. Permeability leakage of BSA-FITC through the cellular monolayer was measured upon the apical administration of 5  $\mu$ M NHBA, C1, C2 or 1  $\mu$ M bradykinin (BK), as positive control. As shown in Fig. 1A, similarly to BK, the C2 fragment increased endothelial permeability already after 15 min, an effect that became stronger after 30 min and even more after 45 min. Notably, neither the C1 fragment nor the full-length protein NHBA were able to produce a similar effect. Moreover, the alteration of the monolayer integrity, which was not due to a toxic effect (Fig. S2), occurred only if the C2 fragment was administrated to the apical side of endothelia, whereas nothing occurred if the exposure was carried out on the baso-lateral side (data not shown). A dose-response carried out with C2, revealed that at 45 min the peptide was capable of altering endothelial permeability already at 500 nM (Fig. 1B), while at 30 min the leakage became statistically significant at 1  $\mu$ M (data not shown). Considering that 5  $\mu$ M was the lowest concentration at which C2 perturbed the endothelium already after 15 min, we decided to adopt this dose for further experiments. When the transendothelial permeability assay was performed in the presence of antibodies raised against the full-length protein (NHBA), against C2 or just against the arginine-rich domain, the C2 effect was strongly prevented. Notably, no inhibition was observed in the presence of isotypic antibodies, raised against an unrelated antigen (Fig. 1C). The inhibition was also observed in the presence of antibodies anti-NHBA-GNA1030, the fusion protein included in the Bexsero<sup>®</sup> MenB vaccine (Donnelly *et al.*, 2010).

## C2 localizes within mitochondria

In order to address how C2 elicited endothelial perturbation, we investigated its sub-cellular localization within host endothelial cells. First, we took advantage of software capable of predicting a possible localization of a peptide within cells. Among these, we used the MitoProt package (<http://ihg.gsf.de/ihg/mitoprot.html>), which defines whether an N-terminal protein region contains a mitochondrial targeting sequence. The software attributes a score value ranging from 1 to 0, depending on whether the sequence analyzed is more or less compatible with mitochondrial localization. In case of C2, MitoProt yielded a score of 0.7152, which strongly suggested a mitochondrial localization. Indeed, the N-terminal domain of C2 is enriched in basic residues (arginines), that usually confer to a protein the ability of targeting mitochondria (von Heijne, 1986). On the contrary, for NHBA and C1, MitoProt yielded a score of 0.205 and 0.0199, respectively. In order to verify whether the bioinformatics prediction was accurate, we incubated HBMECs with C2, before proceeding with the isolation of mitochondrial, microsomal and cytosolic fractions, at different time points. The protein content of all the fractions was analyzed by western blot for evaluating the presence of C2 and possibly defining its intracellular trafficking. Fig. 2A shows that, after 5 min, C2 was detectable both in microsomes and in the cytosol, while, 15 min after its administration, a fraction of C2 accumulated in mitochondria. After 45 min, C2 was entirely confined to the latter organelle. Independently of the sub-cellular localization, C2 always maintained the N-terminal domain, as demonstrated by the fact that the antibodies anti-arginine-rich peptide revealed the protein. Immunofluorescence analysis performed on cells exposed to C2 allowed us to exclude that the peptide localization within mitochondria was due to a co-segregation of C2 with mitochondrial fraction occurring post lysis (Fig. S3).

In order to confirm the specific localization of the C2 fragment within mitochondria, the same sub-cellular fractionation and analysis was carried on HBMECs exposed to C1; as expected, the peptide did not show any accumulation in mitochondria and, additionally, it was undetectable in the other two

1  
2  
3  
4  
5  
6  
7  
8  
9  
10  
11  
12  
13  
14  
15  
16  
17  
18  
19  
20  
21  
22  
23  
24  
25  
26  
27  
28  
29  
30  
31  
32  
33  
34  
35  
36  
37  
38  
39  
40  
41  
42  
43  
44  
45  
46  
47  
48  
49  
50  
51  
52  
53  
54  
55  
56  
57  
58  
59  
60

fractions (Fig. 2A). We excluded that C1 was not detected because of the inability of the antibodies to recognize it: indeed, a western blot performed on recombinant C1, revealed that the latter was recognized similarly to C2 by antibodies against the full-length protein NHBA. (Fig. 2B). This result confirms the crucial role of the arginine domain of C2 for its biological activity and indicates that C1 has poor propensity to interact with the cells (Fig. S3).

**C2 induces mitochondrial ROS production**

The integrity of endothelial barrier can be perturbed by ROS. For instance, it is well documented that VEGF induces ROS production and alters the monolayer integrity of the endothelial tissue. Although the relationship between ROS and endothelial permeability is not fully understood, it is known that the production of intracellular ROS leads to the phosphorylation of VE-cadherin and  $\beta$ -catenin (both proteins of the adherens junctions) (Monaghan-Benson *et al.*, 2009).

The mitochondrial electron transport chain is one of the major cellular generators of reactive oxygen species, which include superoxide, hydrogen peroxide and the hydroxyl free radical (Loschen *et al.*, 1971, Boveris *et al.*, 1972, Chance *et al.*, 1979). Following the observation that C2 localizes in mitochondria, we decided to verify whether the increased endothelial permeability, caused by the fragment, could follow ROS production within the organelle. Microscopic imaging applied to HBMECs, loaded with the fluoroprobe MitoSOX Red, that permits quantitative detection of mitochondrial superoxide production (Mukhopadhyay *et al.*, 2007), showed significant increase in mitochondrial fluorescence intensity in the cells following the administration of C2, but not of C1 (Fig. 3A). As expected, pre-treatment of the cells with the ROS scavenger N-acetylcysteine (NAC) fully prevented the C2-induced fluorescence increase (Fig. 3A).

Mitochondrial H<sub>2</sub>O<sub>2</sub> generation in confluent HBMECs was also evaluated in cells overexpressing mitochondria-targeted HyPer-dMito, which is a fully genetically encoded fluorescent sensor capable of



detecting mitochondrial  $\text{H}_2\text{O}_2$  in a highly specific manner (Belousov *et al.*, 2006). The probe has two excitation peaks at 420 nm and 500 nm and one emission peak at 516 nm. Upon ROS induction, the excitation peak at 420 nm decreases proportionally to the increase of the peak at 500 nm, allowing ratiometric measurements.

As shown in Fig. 3B, the exposure of cells to the C2 fragment was characterized by a fluorescence ratio decrease while, on the contrary, it remained constant following C1 administration as well as in control cells. ROS increase was appreciable in few minutes with both methods, although with different kinetics: this reflects the nature of the probes, MitoSOX and HyPer-dMito, that are irreversibly and reversibly oxidized, respectively (Lukyanov *et al.*, 2013).

In accordance with the previous experiment, the scavenging of  $\text{H}_2\text{O}_2$  by NAC prevented fluorescence ratio decrease (Fig. 3B).

### **Reactive oxygen species are required for C2-induced endothelial permeability alteration**

Next, we wondered whether ROS production induced by C2 was involved in the alteration of the endothelial integrity; in order to address this possibility, we repeated the permeability assays on HBMECs, seeded on Transwell, in the presence or absence of NAC.

The results shown in Fig. 4 reveal that, at any considered time point, the ROS scavenger NAC significantly reduced the passage of BSA-FITC through the monolayer: the accumulation of the marker in the lower chamber of the apparatus was similar to that measured following the application of C1, which, as expected, was insensitive to the presence of the scavenger.

Collectively, these data support the conclusion that perturbation of endothelial cells, due to C2, requires intracellular accumulation of ROS; the latter being mainly produced within mitochondria where C2 localizes.

1  
2  
3  
4  
5  
6  
7  
8  
9  
10  
11  
12  
13  
14  
15  
16  
17  
18  
19  
20  
21  
22  
23  
24  
25  
26  
27  
28  
29  
30  
31  
32  
33  
34  
35  
36  
37  
38  
39  
40  
41  
42  
43  
44  
45  
46  
47  
48  
49  
50  
51  
52  
53  
54  
55  
56  
57  
58  
59  
60

**C2 induces VE-cadherin phosphorylation in a ROS-dependent manner**

It has been reported that VEGF leads to the generation of ROS, which, in turn, elevates the tyrosine phosphorylation of VE-cadherin, ultimately regulating adherens junction integrity (Monaghan-Benson *et al.*, 2009, Lee *et al.*, 2011). VE-cadherin phosphorylation, induced by VEGF and by other mediators, such as histamine and bradykinin, is followed by the internalization and ubiquitination of the junctional protein, leading to the opening of endothelial cells junctions (Andriopoulou *et al.*, 1999, Orsenigo *et al.*, 2012).

We sought to determine if the C2-induced increase in microvascular permeability could be associated with the tyrosine phosphorylation of VE-cadherin. For this purpose, we used endothelial cells derived from murine embryonic stem cells with homozygous null mutation of the VE-cadherin gene and overexpressing wild-type human VE-cadherin (Zanetti *et al.*, 2002). We decided to take advantage of this cell model because of the high expression of the junctional protein with respect to HBMECs. In order to abolish the basal phosphorylation rate that commonly occurs in cells (Vincent *et al.*, 2004), the endothelial monolayer was serum-starved for 24 h before being exposed to C2. After VE-cadherin immunoprecipitation, the phosphorylation state of the protein tyrosines was evaluated by western blot. Fig. 5A shows that, already after 5 min of treatment, VE-cadherin was phosphorylated in cells exposed to the C2 fragment, and the phosphorylation level increased further up to 15 min, before decreasing at 45 min. As expected, when cells overexpressing the junctional protein were pre-treated with NAC, the fragment was no longer able to cause phosphorylation of VE-cadherin (Fig. 5B), suggesting that ROS are required for the phosphorylation of the protein. Notably, pre-treatment of cells with the Src kinase inhibitor SU6656 also fully prevented the phosphorylation of VE-cadherin (Fig. 5B), as already reported for VEGF (Weis *et al.*, 2005). Finally, incubation with anti-C2 antibodies also impaired the effect elicited by C2 (Fig.5B).

## C2 promotes VE-cadherin endocytosis

Phosphorylation of VE-cadherin is associated with the internalization of the junctional protein via the endo-lysosomal pathway (Xiao *et al.*, 2003). Therefore, based on the phosphorylation of VE-cadherin upon the exposure of the cells to C2, we investigated the localization of the junctional protein in the same cells in response to the fragment. We took advantage of a monoclonal antibody (BV6) which recognizes the extracellular domain of VE-cadherin (Gavard *et al.*, 2006). Murine cells overexpressing VE-cadherin were incubated with the antibody at 4°C, to block cellular trafficking, then exposed to C2 for 45 min at 37°C. We chose this time point with the aim to correlate the localization of VE-cadherin with the maximal effect of C2 on the endothelial monolayer integrity. VE-cadherin internalization was monitored by revealing the protein-antibody complex, by applying a secondary antibody in permeabilized cells. Figure 6 shows that C2 stimulation led to the intracellular accumulation of VE-cadherin which acquired a vesicular distribution. In contrast, few sparse vesicles were observed in cells exposed to saline (control). Interestingly, if cells were exposed to C2 in the presence of NAC, the VE-cadherin pattern was similar to that of control, as expected. The absence of any cell-surface staining, independently of the treatment, was due to a mild acid wash, which removed the amount of antibody bound to the membrane-associated VE-cadherin: this approach permitted to better distinguish cell surface cadherin from the internalized one.

## C2 decreases VE-cadherin intracellular content

The observation that VE-cadherin was internalized raised the possibility that it might be also degraded. Therefore, we quantified the total VE-cadherin content in cells exposed to C2 by a cell-based ELISA and by flow cytometry analysis. With the aim of recapitulating and reinforcing the evidence obtained with the murine cells overexpressing VE-cadherin, we returned to the original cell model, feeling confident in the high sensitivity of the two technical approaches. As shown in Figure 7, the exposure of

1  
2  
3  
4  
5  
6  
7  
8  
9  
10  
11  
12  
13  
14  
15  
16  
17  
18  
19  
20  
21  
22  
23  
24  
25  
26  
27  
28  
29  
30  
31  
32  
33  
34  
35  
36  
37  
38  
39  
40  
41  
42  
43  
44  
45  
46  
47  
48  
49  
50  
51  
52  
53  
54  
55  
56  
57  
58  
59  
60

post-confluent HBMECs to C2 for 45 min reduced by about 20% the VE-cadherin content which remained low even if the treatment was extended to 3 h. Notably, NAC pre-treatment almost fully prevented the C2-induced VE-cadherin disappearance (Fig. 7A and D). The same effect was observed in cells exposed to C2 in the presence of anti-C2 antibodies (Fig. 7B and E).

Consistent with the fact that C2 induced phosphorylation of VE-cadherin and that the latter was abolished when Src kinase was inhibited, the blockage of Src by SU6656, before the administration of C2, significantly counteracted VE-cadherin reduction (Fig. 7B and E). Finally, the blockage of the fusion between endosomes and lysosomes by chloroquine, maintained the total cell content of VE-cadherin similar to that of control cells.

Collectively, our data suggest that C2 leads to the generation of ROS, which, in turn, elevate the tyrosine phosphorylation of the junctional protein VE-cadherin. The latter event, probably mediated at least in part by Src kinase, is followed by the endocytosis and subsequent degradation of the protein. The removal of VE-cadherin from the junctional complex is expected to be responsible for the increased permeability of the endothelial monolayers upon exposure to C2.

## Discussion

In this study, we demonstrate that a fragment originating from the cleavage of the Neisserial Heparin Binding Antigen (NHBA), by the bacterial protease NalP and referred to as C2, increases the permeability of endothelial monolayers. Once applied to the apical side of endothelial cells, C2 quickly accumulates in mitochondria where it stimulates the production of oxygen radicals. The specific targeting of C2 resides in its N-terminal arginine-rich domain; indeed, C1, another NHBA-derived fragment resulting from the proteolysis by the human lactoferrin (Serruto *et al.*, 2010) and differing from C2 because it lacks the arginine sequence, does not localize to mitochondria. Our evidence is in accordance with observations made by other authors testifying that arginines improve membrane permeability and mitochondrial accumulation of proteins (Mitchell *et al.*, 2000, Borgese *et al.*, 2001, Zanetti *et al.*, 2002, Nakase *et al.*, 2012). However, the fact that in heparinase-treated HBMEC monolayers the leakage due to C2 was almost completely compromised (data not shown), suggest that proteoglycans are essential at least for the docking of the protein to the plasma membrane.

C1 does not reach mitochondria, it is unable to trigger ROS production, and does not alter endothelial permeability. Therefore, it is plausible that the ability of C2 in affecting the endothelial barrier is related to its subcellular localization and to the accumulation of ROS. Moreover, C2 has to be applied on the apical side of the endothelial monolayer to alter its integrity and this suggests that *in vivo* it could work within the microvasculature when bacteria form microcolonies along the vascular wall or aggregates inside the lumen of blood vessels (Coureuil *et al.*, 2009, Dupin *et al.*, 2012).

The role of ROS in C2-induced perturbation of endothelial permeability became clear when we found that the administration of the fragment to mouse embryonic cells overexpressing VE-cadherin resulted in an increased tyrosine phosphorylation of the protein, which is a major component of the adherens junctions, and that this event was prevented by NAC. These data suggested that C2 could activate a Src kinase by means of ROS; accordingly, it is established that these enzymes are redox-

1  
2  
3  
4  
5  
6  
7  
8  
9  
10  
11  
12  
13  
14  
15  
16  
17  
18  
19  
20  
21  
22  
23  
24  
25  
26  
27  
28  
29  
30  
31  
32  
33  
34  
35  
36  
37  
38  
39  
40  
41  
42  
43  
44  
45  
46  
47  
48  
49  
50  
51  
52  
53  
54  
55  
56  
57  
58  
59  
60

regulated proteins (Giannoni *et al.*, 2010). The fact that, when C2 was administrated to cells previously exposed to a Src inhibitor, VE-cadherin phosphorylation was impaired, definitely strengthened the idea that C2 activates Src and that this is achieved by acting through redox signalling.

We found that C2 decreases by about 20% the VE-cadherin content in HBMECs and this effect is almost fully prevented by both NAC and Src inhibitor. Moreover, we demonstrated that the reduction of the junctional protein relies on its enhanced internalization via the endo-lysosomal pathway, a physiological process culminating in the degradation of VE-cadherin that controls the adhesive properties of the cells (Xiao *et al.*, 2003).

It is established that *N. meningitidis*, having left the upper respiratory tract, reaches the bloodstream where it interacts and modifies the properties of the endothelium by triggering intracellular signalling: this occurs in case of meningitis as well as in case of sepsis-associated *purpura fulminans* and results in an increased paracellular permeability (Coureuil *et al.*, 2013). In both situations it has been demonstrated that the main role is exerted by the type IV pili, at least for the Meningococcus strain C, and the molecular mechanism that involves these structures in perturbing the endothelium is well defined mainly in case of brain microvasculature. Type IV pili initially permit the adhesion of bacteria to the endothelium and subsequently, via a  $\beta$ -adrenoreceptor/ $\beta$ -arrestin pathway, lead to the recruitment of junctional proteins under bacterial colonies, weakening the endothelial barrier and thus permitting the passage of bacteria. The activation of  $\beta$ -arrestin leads also to the recruitment and activation of the kinase Src which is involved in the formation of actin-rich cellular protrusions (Coureuil *et al.*, 2009, Coureuil *et al.*, 2010).

With the present study, we demonstrated that the fragment C2 perturbs endothelial integrity through a Src-dependent pathway. Notably, it was shown that pili expression is downregulated during prolonged infection experiment, once bacteria microcolonies are formed (Morand *et al.*, 2004), therefore it is

1  
2  
3 plausible that a second mechanism, maybe involving C2, contribute to the activity of pili in perturbing  
4  
5 the endothelial barrier.  
6  
7

8 In conclusion, with this study we demonstrate that the NHBA-derived fragment C2 alters endothelial  
9  
10 permeability causing vascular leakage, a clinical feature particularly evident in the case of  
11  
12 meningococemia with high bacteremia and purpuric lesions (Coureuil *et al.*, 2013). The recent setting  
13  
14 up of an animal model for meningococcal infection, in which human skin is xenografted into  
15  
16 SCID/beige mice (Melican *et al.*, 2013), would be useful for confirming the impact of NHBA-derived  
17  
18 C2 during the meningococcus-related diseases.  
19  
20  
21  
22  
23  
24  
25  
26  
27  
28  
29  
30  
31  
32  
33  
34  
35  
36  
37  
38  
39  
40  
41  
42  
43  
44  
45  
46  
47  
48  
49  
50  
51  
52  
53  
54  
55  
56  
57  
58  
59  
60

1  
2  
3  
4  
5  
6  
7  
8  
9  
10  
11  
12  
13  
14  
15  
16  
17  
18  
19  
20  
21  
22  
23  
24  
25  
26  
27  
28  
29  
30  
31  
32  
33  
34  
35  
36  
37  
38  
39  
40  
41  
42  
43  
44  
45  
46  
47  
48  
49  
50  
51  
52  
53  
54  
55  
56  
57  
58  
59  
60

## Experimental Procedures

### *Reagents*

Phosphate-buffered saline (PBS), D-MEM High Glucose and Foetal bovine serum (FBS) were purchased from Euroclone. Gentamicin and Hepes were purchased from Gibco. Endothelial cells growth supplement (ECGS), BSA-FITC, Red Ponceau, tetramethylbenzidine (TMB) and TMB Stop Solution (1 M sulphuric acid), MEM non essential aminoacids, MEM vitamins, BSA, type-B gelatine, N-acetylcysteine (NAC), DTT, mouse control serum and Tween-20 were obtained from Sigma-Aldrich. Nitrocellulose membrane, 5-ml His Trap HPcolumn, X-ray film and ECL (enhanced chemiluminescence system) were purchased from GE Healthcare. BCA protein assay reagent was purchased from Pierce. Mitosox Red, Alexa Fluor 488-conjugated anti mouse secondary antibody and Alexa Fluor 594-conjugated anti rabbit secondary antibody, 4-12% and 10% SDS-PAGE gels, LDS 4X sample buffer, NuPAGE antioxidant, NuPAGE MES 20X Running Buffer, NuPAGE 20x Transfer Buffer were obtained from Invitrogen. VEGF was obtained from Immunological Sciences. Mitochondria Isolation kit and QiAMP mini-prep Kit were purchased from Qiagen. SU6656, monoclonal anti-GAPDH antibody and monoclonal anti-Ve-cadherin (BV6) were purchased from Merck-Millipore. Rabbit polyclonal anti-TOM20, goat polyclonal antibody labelled with phycoerythrin (PE) anti VE-cadherin, goat polyclonal and monoclonal anti-VE-cadherin antibodies and agarose-coupled Protein G and A were from Santa Cruz Biotechnology. Rabbit polyclonal antibody against EEA1 was from Abcam and monoclonal antibody against phosphotyrosine (clone G410) was obtained from Upstate Biotechnolgy. Monoclonal antibody anti-respiratory chain complex II (COX II) was purchased form Mitoscience. 8-well chambers slide and NU-serum IV were obtained from BD Bioscences. Annexin-V conjugated to Alexa 488 was purchased from Bender MedSystem.



## Cell culture

Simian virus 40 large T antigen-transformed human brain microvascular endothelial cells (HBMEC) were kindly provided by Novartis Vaccines and Diagnostics s.r.l. (Siena, Italy) and were cultured in T75 flasks, in FBS/NU-serum IV-supplemented DMEM high glucose plus non-essential aminoacids and vitamins, to a confluent monolayer. For *in vitro* permeability assays, cells were split and seeded on gelatine-coated Transwell cell culture chambers (polycarbonate filters, 0.3  $\mu\text{m}$  or 3  $\mu\text{m}$  pore size; Corning Costar Corporation, Cambridge, MA, USA) at a density of  $7 \times 10^4$  cells per well. Cells were grown for 5 days before performing permeability assays.

Endothelial cells derived from murine embryonic stem cells with homozygous null mutation of the VE-cadherin gene and overexpressing wild-type human VE-cadherin (Lampugnani *et al.*, 2002, Grazia Lampugnani *et al.*, 2003) were kindly provided by E. Dejana (IFOM, Milan, Italy). Cells were maintained in culture in T75 flasks in FBS-supplemented DMEM high glucose plus heparin and ECGS.

## Preparation of antisera and IgG purification

Preparation of anti-NHBA, anti-NHBA-GNA1030, anti-C1 and anti-C2 sera is described elsewhere (Serruto *et al.*, 2010). The peptide CSFARFRRSARSRR, corresponding to the arginine-rich domain at the N-terminus of C2 plus a terminal cysteine, was conjugated to Keyhole Limpet Hemocyanin (KLH) using an Inject Activated Immunogen Conjugation Kit (Pierce) and injected into rabbits. The anti-peptide antibodies generated (referred to as anti-Arg-seq) were purified by affinity chromatography on SulfoLink coupling gels (Pierce) onto which the peptide was conjugated. Animal protocols were approved by the local animal ethical committee and by the Italian Minister of Health in accordance with Italian law.

Polyclonal IgG were purified from mouse control serum and from antisera using a mix of Sepharose A and G beads. Briefly, sera were diluted to 1 ml in binding buffer (1.5 M Glycine/NaOH, pH 9.0, 3 M

1  
2  
3  
4  
5  
6  
7  
8  
9  
10  
11  
12  
13  
14  
15  
16  
17  
18  
19  
20  
21  
22  
23  
24  
25  
26  
27  
28  
29  
30  
31  
32  
33  
34  
35  
36  
37  
38  
39  
40  
41  
42  
43  
44  
45  
46  
47  
48  
49  
50  
51  
52  
53  
54  
55  
56  
57  
58  
59  
60

NaCl), added to the Sepharose beads mix and incubated overnight on an end-over shaker at 4°C. IgG were eluted in 150 µl of elution buffer (0.2 M Glycine/HCl buffer pH 2.5) and neutralized with neutralization buffer (1 M Tris/HCl, pH 9.0). A final concentration of 250 µg/ml of isolated IgG was used in the permeability assays, considering a concentration of specific antibodies of about 10% of total IgG (25 µg/ml).

*Construction of plasmids and protein expression*

For the expression of all the recombinant proteins considered in this study, the specific DNA fragments were amplified by PCR from *N. meningitidis* MC58 genomic DNA and cloned into the pET-21b+ expression vector (Invitrogen), as detailed elsewhere (Serruto *et al.*, 2010). Purification of recombinant NHBA and of recombinant fragments C1 and C2 have also been previously reported (Serruto *et al.*, 2010). SE-UPLC (size exclusion chromatography) and RP-HPLC (reverse phase chromatography) applied to the purified peptides revealed a purity of greater than or equal to 93%.

*Permeability assays*

HBMECs were seeded onto 2% gelatine-coated Transwell filters (0.3 µm pore size) at the density of 7 × 10<sup>4</sup> cells per well in a 24-well plate. Cells were used 5 days after seeding onto filters. The formation of intact monolayer on the insert was evaluated by adding FITC-BSA (1 mg/ml) to the upper chamber and measuring after 5 min the amount of labelled BSA passed into the lower chamber by a Fluostar microplate reader (SLT Labinstruments). Transwells were used only when the intensity of fluorescence in the lower chamber was negligible; in this case, the stimuli were added to the upper chamber together with FITC-BSA, and the fluorescence was evaluated in the lower chamber at various time intervals. Calibration curves were set up measuring the fluorescence intensity of increasing concentrations of

FITC-BSA. When required, cells were exposed to 1 mM N-acetylcysteine (NAC) 30 min before adding the stimuli. For evaluating the blocking activity of antibodies anti-NHBA, anti-NHBA-GNA1030, anti-C2 and anti-Arg sequence, they were singularly preincubated with C2 (1 h at 37°C) before addition to the endothelial monolayers. Isotypic antibodies were applied as negative control.

### *Cell viability assay*

Cells were incubated with the phosphatidylserine-binding protein Annexin-V conjugated to Alexa 488, according to the manufacturer's instructions. Viability was measured by flow cytometry (FACSCalibur, BD Biosciences, San Jose, CA, USA) and expressed as percentage of Annexin-V-negative events in the gated population.

### *Mitochondria isolation*

HBMECs were seeded onto T75 flasks and, once confluent, were exposed to 5  $\mu$ M C1 or C2 for 5, 15 and 45 min. Cells were collected, washed in ice-cold PBS and processed by Qiagen Mitochondria Isolation Kit. Protein content of isolated fractions, corresponding to mitochondria, cytosol and microsomal fraction, was determined by BCA assay. 10  $\mu$ g of each fraction were loaded on SDS-PAGE 4-12% and analyzed by western blot.

### *Immunoprecipitation*

Murine endothelial cells overexpressing wild-type human VE-cadherin were grown in T75 flasks. Cell layers were serum-starved for 1 day before the application of stimuli. 5  $\mu$ M C2 was added for 5, 15 and 45 min. Anti-C2 antibody was used at the final concentration of 25  $\mu$ g/ml. When required, cells were pre-incubated for 30 min with 1 mM NAC or with 280 nM SU6656. Cells, detached by scraping, were

1  
2  
3  
4  
5  
6  
7  
8  
9  
10  
11  
12  
13  
14  
15  
16  
17  
18  
19  
20  
21  
22  
23  
24  
25  
26  
27  
28  
29  
30  
31  
32  
33  
34  
35  
36  
37  
38  
39  
40  
41  
42  
43  
44  
45  
46  
47  
48  
49  
50  
51  
52  
53  
54  
55  
56  
57  
58  
59  
60

collected, washed in ice-cold PBS and lysed in 1% (vol/vol) Triton X-100 in 20 mM Tris-HCl, pH 8.0, and 150 mM NaCl (supplemented with 0.2 mg/mL Na orthovanadate, 1 mg/mL pepstatin, leupeptin, and aprotinin and 10 mM PMSF). Post-nuclear supernatants were immunoprecipitated using 2 µg goat polyclonal anti-VE-cadherin coupled to protein G agarose. Immunoprecipitates were resolved by SDS-PAGE. Phosphorylated VE-cadherin was revealed using an anti-phosphotyrosine antibody followed by peroxidase-labeled secondary antibodies according to the manufacturer's instructions. A goat polyclonal antibody anti-total VE cadherin was used as control for equal loading. Western blots were developed by ECL (Thermo, Fisher Scientific).

*Measurement of changes in mitochondrial ROS production in HBMECs*

HBMECs were grown on 24 mm diameter glass dishes until confluence; the medium was removed and replaced with HBSS buffer plus  $\text{Ca}^{2+}$  and  $\text{Mg}^{2+}$ , 10 mM Glucose and 4 mM Hepes. Cells were incubated for 30 min with 1 mM Mitosox Red, before starting the live imaging recording. Imaging was performed with an inverted microscope (Olympus IX50); fluorescence emission at 560 nm, upon excitation at 514 nm, was recorded; images were acquired every 10 seconds with a 60X, 1.4 NA oil immersion objective (Olympus) using the Cell<sup>R</sup> software. Stimuli added were 5 µM C1 or C2; when required, cells were pre-treated 30 min with 1 mM NAC. Data were expressed as  $F/F_0$ , where F is the fluorescence emission intensity at time t and  $F_0$  is the fluorescence emission intensity at time = 0.

Mitochondrial  $\text{H}_2\text{O}_2$  generation in confluent HBMECs was also evaluated in cells transfected with 2 µg of mitochondria-targeted HyPer-Mito (Evrogen, [www.evrogen.com](http://www.evrogen.com)), which is a fully genetically encoded fluorescent sensor capable for highly specific detection of mitochondrial  $\text{H}_2\text{O}_2$  (Belousov *et al.*, 2006). Following the application of stimuli (5 µM C1 or C2), in HBSS buffer plus  $\text{Ca}^{2+}$  and  $\text{Mg}^{2+}$ , 10 mM glucose, 4 mM Hepes, fluorescence emission at 516 nm was recorded (10 s intervals) using an Olympus IX81 microscope following excitation at 420 nm and 500 nm. When required, cells were pre-

1  
2  
3 treated 30 min with 1 mM NAC. The ratio (R) between the emission values at the two wavelengths of  
4  
5 excitation (420/500) was calculated. Data were expressed as  $R/R_0$ , where R is the ratio at time t and  $R_0$   
6  
7 is the ratio at time = 0.  
8  
9

### 10 11 12 13 *Immunofluorescence*

14  
15 HBMECs seeded ( $0.5 \times 10^4$ /ml) on 8-well chamber slides (BD Biosciences) were exposed to C1 or C2  
16  
17 for 45 min. Cells were then fixed with 3.7% formaldehyde in PBS for 30 min, permeabilized with  
18  
19 0.01% Nonidet P40 in PBS for 20 min at RT and blocked with PBS 0.5% BSA. TOM20, adopted as  
20  
21 mitochondrial marker, was revealed with a rabbit polyclonal antibody followed by an ALEXA 594-  
22  
23 conjugated anti-rabbit secondary antibody. C1 or C2 were revealed with polyclonal antibodies purified  
24  
25 from sera of C1 or C2-immunized mice, followed by ALEXA 488-conjugated anti-mouse secondary  
26  
27 antibodies.  
28  
29  
30  
31

### 32 33 34 35 *VE-cadherin internalization assay*

36  
37 The assay was performed using a procedure adapted from a previous report (Paterson *et al.*, 2003).  
38  
39 Murine endothelial cells overexpressing wild-type human VE-cadherin were seeded on 8-well chamber  
40  
41 slides ( $0.5 \times 10^4$ /ml). Cells were exposed for 1 h at 4°C to a monoclonal antibody directed against the  
42  
43 VE-cadherin extracellular domain (BV6), diluted in DMEM 20 mM Hepes, 3% BSA. When required, 1  
44  
45 mM NAC was added 30 min before removing the antibody. Unbound antibody was washed-out by  
46  
47 rinsing cells in ice-cold DMEM 20 mM Hepes, 3% BSA. Cells were incubated with 5  $\mu$ M C2 for 45  
48  
49 min at 37 °C in the same medium; where required, NAC was renewed. Cells exposed to saline  $\pm$  NAC  
50  
51 were used as controls. To remove cell surface bound antibody, while retaining internalized antibody,  
52  
53 cells were washed for 15 min in PBS, pH 2.7 containing 25 mM glycine and 3% BSA. Cells were fixed  
54  
55  
56  
57  
58  
59  
60

1  
2  
3  
4  
5  
6  
7  
8  
9  
10  
11  
12  
13  
14  
15  
16  
17  
18  
19  
20  
21  
22  
23  
24  
25  
26  
27  
28  
29  
30  
31  
32  
33  
34  
35  
36  
37  
38  
39  
40  
41  
42  
43  
44  
45  
46  
47  
48  
49  
50  
51  
52  
53  
54  
55  
56  
57  
58  
59  
60

with 3.7% formaldehyde in PBS for 30 min, permeabilized with 0.01% Triton X-100 0.5% in PBS for 15 min at RT. The internalized VE-cadherin, complexed with the antibody, was revealed with an ALEXA 488-conjugated anti-mouse secondary antibody, while nuclei were revealed with DAPI. Cells were visualized with a 63X oil immersion objective on a laser-scanning confocal microscope and images were acquired using the LAS-AF software (Leica TCS-SP5, Leica Microsystems, Wetzlar, Germany). Images were then processed using ImageJ (Research Services Branch, National Institute of Mental Health, Bethesda, MD, USA).

*Cell-based ELISA for evaluation of VE-cadherin content*

Cell-based ELISA was performed as previously reported (Shen *et al.*, 2011) with minor modifications. Briefly, HBMECs were seeded ( $5 \times 10^4$ /well) onto 96-well plates. Three days after reaching confluence and forming a contact-inhibited monolayer, cells were treated with 5  $\mu$ M C2 for 45 min or 3 h. When required, cells were pre-treated for 30 min with 1 mM NAC, 280 nM SU6656 or 100  $\mu$ M chloroquine for 2 h. For evaluating the effect of anti-C2 antibodies, the latter were added together with C2 at a final concentration of 250  $\mu$ g/ml. Cells were fixed with 3.7% formaldehyde for 10 min at RT and incubated with blocking buffer (PBS with 10% FBS) for 60 min at 37°C. After washing with 0.1% Triton X-100 in PBS, cells were incubated with a goat polyclonal antibody against VE-cadherin (1:500) overnight at 4°C. After washing with PBS, a secondary HRP-conjugated antibody was added and incubated for 1 h at RT. After washing again, TMB solution was added, incubated for 15 min followed by the stop solution for 5 min. The optical density of each well was read at 450 nm using a plate reader (Tecan, Infinite 200 pro, Salzburg, Austria). Results were expressed as percentage of the control group (cells exposed to saline).

### *Flow cytometry for evaluation of VE-cadherin content*

HBMECs were seeded ( $2 \times 10^5$ /well) in 24-well plates. Three days after reaching confluence and forming a contact-inhibited monolayer, cells were treated with 5  $\mu$ M C2 for 45 min or 3 h. When required, cells were pre-treated with NAC, SU6656 or chloroquine as detailed above. 250  $\mu$ g/ml anti-C2 antibodies were added to the cells together with C2.

Cells were detached with 2 mM Na-EDTA and collected in flow cytometry tube. After washing in PBS, cells were pelleted at 1200 rpm for 5 min at 4°C and fixed and permeabilized with ice-cold methanol in ice for 30 min. A PE-conjugated anti-VE-cadherin antibody was used to label the cytosolic portion of the protein. Cells were analyzed by flow cytometry (FACSCalibur) and data analysis was carried out using CellQuest software (BD Biosciences).

### *Statistical analyses*

Statistical significance was calculated by unpaired Student's *t*-test. Data, reported as the mean  $\pm$  S.D., were considered significant if *p*-values  $\leq 0.05$ .

1  
2  
3  
4  
5  
6  
7  
8  
9  
10  
11  
12  
13  
14  
15  
16  
17  
18  
19  
20  
21  
22  
23  
24  
25  
26  
27  
28  
29  
30  
31  
32  
33  
34  
35  
36  
37  
38  
39  
40  
41  
42  
43  
44  
45  
46  
47  
48  
49  
50  
51  
52  
53  
54  
55  
56  
57  
58  
59  
60

**Acknowledgements**

We thank L. Santini and F. Ferlicca (Novartis Vaccines and Diagnostics) for providing all the sera, E. Martinelli, M. Giuliani, E. Cartocci and E. Grassi (Novartis Vaccines and Diagnostics) for preparation and purification of recombinant C2 protein and V. Massignani (Novartis Vaccines and Diagnostics) and C. Giampietro (IFOM-IEO Campus) for helpful discussion and advices. This work was partially supported by Italian Ministry of University and Research, Prin projects and Fondazione Cariplo, grant N° 2011-0485 (to MdB).

The authors declare that no conflict of interest exists.



## References

- Andriopoulou, P., Navarro, P., Zanetti, A., Lampugnani, M.G. and Dejana, E. (1999). Histamine induces tyrosine phosphorylation of endothelial cell-to-cell adherens junctions. *Arteriosclerosis, thrombosis, and vascular biology* **19**, 2286-2297.
- Belousov, V.V., Fradkov, A.F., Lukyanov, K.A., Staroverov, D.B., Shakhbazov, K.S., Terskikh, A.V. and Lukyanov, S. (2006). Genetically encoded fluorescent indicator for intracellular hydrogen peroxide. *Nature methods* **3**, 281-286.
- Borgese, N., Gazzoni, I., Barberi, M., Colombo, S. and Pedrazzini, E. (2001). Targeting of a tail-anchored protein to endoplasmic reticulum and mitochondrial outer membrane by independent but competing pathways. *Molecular biology of the cell* **12**, 2482-2496.
- Boveris, A., Oshino, N. and Chance, B. (1972). The cellular production of hydrogen peroxide. *The Biochemical journal* **128**, 617-630.
- Caesar, N.M., Myers, K.A. and Fan, X. (2013). Neisseria meningitidis serogroup B vaccine development. *Microb Pathog* **57**, 33-40.
- Chance, B., Sies, H. and Boveris, A. (1979). Hydroperoxide metabolism in mammalian organs. *Physiological reviews* **59**, 527-605.
- Chen, T., Swanson, J., Wilson, J. and Belland, R.J. (1995). Heparin protects Opa+ Neisseria gonorrhoeae from the bactericidal action of normal human serum. *Infection and immunity* **63**, 1790-1795.
- Coureuil, M., Join-Lambert, O., Lecuyer, H., Bourdoulous, S., Marullo, S. and Nassif, X. (2013). Pathogenesis of meningococemia. *Cold Spring Harb Perspect Med* **3**.
- Coureuil, M., Lecuyer, H., Scott, M.G., Boularan, C., Enslen, H., Soyer, M., et al. (2010). Meningococcus Hijacks a beta2-adrenoceptor/beta-Arrestin pathway to cross brain microvasculature endothelium. *Cell* **143**, 1149-1160.
- Coureuil, M., Mikaty, G., Miller, F., Lecuyer, H., Bernard, C., Bourdoulous, S., et al. (2009). Meningococcal type IV pili recruit the polarity complex to cross the brain endothelium. *Science* **325**, 83-87.
- de Vries, F.P., Cole, R., Dankert, J., Frosch, M. and van Putten, J.P. (1998). Neisseria meningitidis producing the Opc adhesin binds epithelial cell proteoglycan receptors. *Molecular microbiology* **27**, 1203-1212.
- Donnelly, J., Medini, D., Boccadifuoco, G., Biolchi, A., Ward, J., Frasc, C., et al. (2010). Qualitative and quantitative assessment of meningococcal antigens to evaluate the potential strain coverage of protein-based vaccines. *Proc Natl Acad Sci U S A* **107**, 19490-19495.
- Dupin, N., Lecuyer, H., Carlotti, A., Poyart, C., Coureuil, M., Chanal, J., et al. (2012). Chronic meningococemia cutaneous lesions involve meningococcal perivascular invasion through the remodeling of endothelial barriers. *Clin Infect Dis* **54**, 1162-1165.
- Gallagher, J.T., and Lyon, M. (2000) Molecular structure of heparan sulfate and interactions with growth factors and morphogens. In *Proteoglycans: structure, biology and molecular interactions*. , R.V. Iozzo (ed.). New York, Marcel Dekker Inc. New York, pp. 27-59.
- Gavard, J. and Gutkind, J.S. (2006). VEGF controls endothelial-cell permeability by promoting the beta-arrestin-dependent endocytosis of VE-cadherin. *Nat Cell Biol* **8**, 1223-1234.
- Giannoni, E., Taddei, M.L. and Chiarugi, P. (2010). Src redox regulation: again in the front line. *Free radical biology & medicine* **49**, 516-527.
- Grazia Lampugnani, M., Zanetti, A., Corada, M., Takahashi, T., Balconi, G., Breviario, F., et al. (2003). Contact inhibition of VEGF-induced proliferation requires vascular endothelial cadherin, beta-catenin, and the phosphatase DEP-1/CD148. *The Journal of cell biology* **161**, 793-804.
- Iozzo, R.V. (1998). Matrix proteoglycans: from molecular design to cellular function. *Annual review of biochemistry* **67**, 609-652.

1  
2  
3  
4  
5  
6  
7  
8  
9  
10  
11  
12  
13  
14  
15  
16  
17  
18  
19  
20  
21  
22  
23  
24  
25  
26  
27  
28  
29  
30  
31  
32  
33  
34  
35  
36  
37  
38  
39  
40  
41  
42  
43  
44  
45  
46  
47  
48  
49  
50  
51  
52  
53  
54  
55  
56  
57  
58  
59  
60

Lampugnani, M.G., Zanetti, A., Breviario, F., Balconi, G., Orsenigo, F., Corada, M., *et al.* (2002). VE-cadherin regulates endothelial actin activating Rac and increasing membrane association of Tiam. *Molecular biology of the cell* **13**, 1175-1189.

Lee, M., Choy, W.C. and Abid, M.R. (2011). Direct sensing of endothelial oxidants by vascular endothelial growth factor receptor-2 and c-Src. *PloS one* **6**, e28454.

Loschen, G., Flohe, L. and Chance, B. (1971). Respiratory chain linked H<sub>2</sub>O<sub>2</sub> production in pigeon heart mitochondria. *FEBS letters* **18**, 261-264.

Lukyanov, K.A. and Belousov, V.V. (2013). Genetically encoded fluorescent redox sensors. *Biochim Biophys Acta*.

Melican, K., Michea Veloso, P., Martin, T., Bruneval, P. and Dumenil, G. (2013). Adhesion of *Neisseria meningitidis* to dermal vessels leads to local vascular damage and purpura in a humanized mouse model. *PLoS Pathog* **9**, e1003139.

Menozzi, F.D., Rouse, J.H., Alavi, M., Laude-Sharp, M., Muller, J., Bischoff, R., *et al.* (1996). Identification of a heparin-binding hemagglutinin present in mycobacteria. *The Journal of experimental medicine* **184**, 993-1001.

Mitchell, D.J., Kim, D.T., Steinman, L., Fathman, C.G. and Rothbard, J.B. (2000). Polyarginine enters cells more efficiently than other polycationic homopolymers. *The journal of peptide research : official journal of the American Peptide Society* **56**, 318-325.

Monaghan-Benson, E. and BurrIDGE, K. (2009). The regulation of vascular endothelial growth factor-induced microvascular permeability requires Rac and reactive oxygen species. *The Journal of biological chemistry* **284**, 25602-25611.

Morand, P.C., Bille, E., Morelle, S., Eugene, E., Beretti, J.L., Wolfgang, M., *et al.* (2004). Type IV pilus retraction in pathogenic *Neisseria* is regulated by the PilC proteins. *EMBO J* **23**, 2009-2017.

Mukhopadhyay, P., Rajesh, M., Hasko, G., Hawkins, B.J., Madesh, M. and Pacher, P. (2007). Simultaneous detection of apoptosis and mitochondrial superoxide production in live cells by flow cytometry and confocal microscopy. *Nature protocols* **2**, 2295-2301.

Nakase, I., Okumura, S., Katayama, S., Hirose, H., Pujals, S., Yamaguchi, H., *et al.* (2012). Transformation of an antimicrobial peptide into a plasma membrane-permeable, mitochondria-targeted peptide via the substitution of lysine with arginine. *Chem Commun (Camb)* **48**, 11097-11099.

Orsenigo, F., Giampietro, C., Ferrari, A., Corada, M., Galaup, A., Sigismund, S., *et al.* (2012). Phosphorylation of VE-cadherin is modulated by haemodynamic forces and contributes to the regulation of vascular permeability in vivo. *Nat Commun* **3**, 1208.

Ovstebo, R., Brandtzaeg, P., Brusletto, B., Haug, K.B., Lande, K., Hoiby, E.A. and Kierulf, P. (2004). Use of robotized DNA isolation and real-time PCR to quantify and identify close correlation between levels of *Neisseria meningitidis* DNA and lipopolysaccharides in plasma and cerebrospinal fluid from patients with systemic meningococcal disease. *J Clin Microbiol* **42**, 2980-2987.

Paterson, A.D., Parton, R.G., Ferguson, C., Stow, J.L. and Yap, A.S. (2003). Characterization of E-cadherin endocytosis in isolated MCF-7 and chinese hamster ovary cells: the initial fate of unbound E-cadherin. *J Biol Chem* **278**, 21050-21057.

Pathan, N., Faust, S.N. and Levin, M. (2003). Pathophysiology of meningococcal meningitis and septicaemia. *Arch Dis Child* **88**, 601-607.

Serruto, D., Bottomley, M.J., Ram, S., Giuliani, M.M. and Rappuoli, R. (2012). The new multicomponent vaccine against meningococcal serogroup B, 4CMenB: immunological, functional and structural characterization of the antigens. *Vaccine* **30 Suppl 2**, B87-97.

Serruto, D., Spadafina, T., Ciucchi, L., Lewis, L.A., Ram, S., Tontini, M., *et al.* (2010). *Neisseria meningitidis* GNA2132, a heparin-binding protein that induces protective immunity in humans. *Proceedings of the National Academy of Sciences of the United States of America* **107**, 3770-3775.

Shen, W., Li, S., Chung, S.H., Zhu, L., Stayt, J., Su, T., *et al.* (2011). Tyrosine phosphorylation of VE-cadherin and claudin-5 is associated with TGF-beta1-induced permeability of centrally derived vascular endothelium. *European journal of cell biology* **90**, 323-332.

- 1  
2  
3 Vincent, P.A., Xiao, K., Buckley, K.M. and Kowalczyk, A.P. (2004). VE-cadherin: adhesion at arm's length.  
4 *American journal of physiology. Cell physiology* **286**, C987-997.  
5  
6 von Heijne, G. (1986). Mitochondrial targeting sequences may form amphiphilic helices. *The EMBO journal* **5**,  
7 1335-1342.  
8  
9 Weis, S.M. and Cheresh, D.A. (2005). Pathophysiological consequences of VEGF-induced vascular permeability.  
10 *Nature* **437**, 497-504.  
11  
12 Xiao, K., Allison, D.F., Kottke, M.D., Summers, S., Sorescu, G.P., Faundez, V. and Kowalczyk, A.P. (2003).  
13 Mechanisms of VE-cadherin processing and degradation in microvascular endothelial cells. *The Journal*  
14 *of biological chemistry* **278**, 19199-19208.  
15  
16 Zanetti, A., Lampugnani, M.G., Balconi, G., Breviario, F., Corada, M., Lanfranccone, L. and Dejana, E. (2002).  
17 Vascular endothelial growth factor induces SHC association with vascular endothelial cadherin: a  
18 potential feedback mechanism to control vascular endothelial growth factor receptor-2 signaling.  
19 *Arteriosclerosis, thrombosis, and vascular biology* **22**, 617-622.  
20  
21  
22  
23  
24  
25  
26  
27  
28  
29  
30  
31  
32  
33  
34  
35  
36  
37  
38  
39  
40  
41  
42  
43  
44  
45  
46  
47  
48  
49  
50  
51  
52  
53  
54  
55  
56  
57  
58  
59  
60

1  
2  
3  
4  
5  
6  
7  
8  
9  
10  
11  
12  
13  
14  
15  
16  
17  
18  
19  
20  
21  
22  
23  
24  
25  
26  
27  
28  
29  
30  
31  
32  
33  
34  
35  
36  
37  
38  
39  
40  
41  
42  
43  
44  
45  
46  
47  
48  
49  
50  
51  
52  
53  
54  
55  
56  
57  
58  
59  
60

**Figure Legends**

**Fig. 1.** The C2 fragment induces the leakage of HBMECs-formed monolayer.

A. Human brain microvascular endothelial cells (HBMECs), grown as monolayer onto the membrane of a Transwell system, were stimulated with 5  $\mu$ M C2, C1, NHBA, or saline (control). 1  $\mu$ M bradikinin (BK) was used as positive control. The passage of FITC-BSA into the lower chamber, at various time intervals, was evaluated.

B. HBMEC monolayers were exposed to the indicated concentrations of C2 for 45 min. Monolayer leakage was evaluated as in A.

C. HBMEC monolayers were exposed to C2 for 45 min in the presence of the indicated antibodies. Monolayer leakage was evaluated as in A. Values are expressed as means  $\pm$  SD of duplicate determinations of four separate experiments. \*,  $p < 0.05$ ; \*\*,  $p < 0.01$ ; \*\*\*,  $p < 0.001$ .

**Fig. 2.** The C2 fragment accumulates in mitochondria.

A. HBMECs, grown to confluence in a T75 flask, were exposed to 5  $\mu$ M C2, C1 or saline (control). After 5, 15 and 45 min mitochondrial (Mt), microsomal (Mf) and cytosolic (C) fractions were isolated and processed for western blot analysis. A mouse polyclonal anti-NHBA antibody was used to reveal both C1 and C2 peptides. The latter was also revealed by a polyclonal antibody specific for the arginine-rich domain. Monoclonal antibodies anti-COXII, anti-EEA1 and anti-GAPDH were used to check the purity of each fraction. HRP-conjugated secondary antibodies were used before developing in chemiluminescence. The molecular weights of the single proteins are in brackets.

B. Control of the ability of anti-NHBA antibody to recognize the C1 peptide. 0.5  $\mu$ g of C1 and C2 were loaded in SDS-PAGE and processed for western blot as in A, using both anti-NHBA and anti-arginine sequence antibodies. The lower band of C2, not recognized by the anti-arginine sequence, is probably a degradation product of the peptide.

**Fig. 3.** C2 induces mitochondrial ROS formation in HBMECs.

A. HBMECs, grown as monolayer, were loaded with 1  $\mu$ M MitoSOX Red, just before live-imaging recording. At the indicated time point (arrow head) cells were exposed to 5  $\mu$ M C1, C2, or saline (control).

When required, cells were pre-treated with 1 mM NAC before being exposed to C2. Cells were excited by laser at 514 nm and fluorescence emitted was recorded at 560 nm every 10 s for 30 min. Data are expressed as  $F/F_0$ , where  $F$  is the fluorescence emission intensity at time  $t$  and  $F_0$  is the fluorescence emission intensity at time = 0. Each kinetics trace is the average of the recording for 3 cells and it is representative of 3 independent experiments performed on different cell preparations. The right panel reports the mean  $\Delta F/F_0 \pm$  SD for the 3 experiments, calculated at 30 min ( $N=3$  cells per experiment).

B. HBMECs, grown as monolayer, were transfected with the Hyper-dMito vector. After 24 h of expression, cells were exposed to 5  $\mu$ M C1, C2, or saline (control). When required, cells were pre-treated with 1 mM NAC before being exposed to C2. Fluorescence intensities were recorded every 10 s for 1 h. Normalized fluorescence ratio changes (420/500 nm) were calculated as a measure of  $H_2O_2$  production. Data are expressed as  $R/R_0$ , where  $R$  is the ratio at time  $t$  and  $R_0$  is the ratio at time = 0. Each kinetics trace is the average of the recording for 3 cells and it is representative of 3 independent experiments performed on different cell preparations. The right panel reports the mean  $\Delta R/R_0 \pm$  SD for the 3 experiments, calculated at 30 min ( $N=3$  cells per experiment). \*\*\*,  $p < 0.001$ .

**Fig. 4.** ROS induced by C2 are essential for the alteration of endothelial permeability.

HBMECs, seeded onto the membrane of a Transwell system, were exposed to 5  $\mu$ M C2 or C1 fragment together with FITC-BSA. When required, HBMECs were pre-treated with 1 mM NAC for 30 min. The accumulation of BSA in the lower chamber was performed as detailed in Figure 1. Values are

1  
2  
3  
4  
5  
6  
7  
8  
9  
10  
11  
12  
13  
14  
15  
16  
17  
18  
19  
20  
21  
22  
23  
24  
25  
26  
27  
28  
29  
30  
31  
32  
33  
34  
35  
36  
37  
38  
39  
40  
41  
42  
43  
44  
45  
46  
47  
48  
49  
50  
51  
52  
53  
54  
55  
56  
57  
58  
59  
60

expressed as mean  $\pm$  SD of duplicate determinations of four separate experiments. \*,  $p < 0.05$ ; \*\*,  $p < 0.01$ .

**Fig. 5.** C2 induces VE-cadherin phosphorylation.

A. Murine endothelial cells overexpressing wild-type human VE-cadherin were grown to confluence before being serum-starved for 24 h and exposed or not to 5  $\mu$ M C2. After 5, 15 and 45 min, cells were harvested and processed for immunoprecipitation with a polyclonal antibody anti-VE-cadherin. Control is represented by cells exposed to saline for 15 min. Phosphorylation state of the protein was determined in western blot by developing with anti-phosphotyrosine antibody. Total VE-cadherin was used as loading control.

B. Cells were pre-treated or not with NAC or with the Src kinase inhibitor SU6656 for 30 min before the administration of C2. C2 was tested either as such or in the presence of anti-C2 antibodies. Control is represented by cells exposed to saline for 45 min.

**Fig. 6.** C2 induces VE-cadherin internalization.

Murine endothelial cells overexpressing wild-type human VE-cadherin were grown to confluence. To evaluate the internalization of the cell surface-associated VE-cadherin, the junctional protein was labelled at 4°C with a monoclonal antibody specific for the extracellular domain. After C2 exposure for 45 min at 37°C, cells were processed for immunofluorescence revealing the protein-antibody complex by an appropriate secondary antibody. Where required, cells were pre-treated with 1 mM NAC for 30 min. Confocal images were acquired using a Leica microscope with a 63 $\times$  oil immersion objective. Images were merged using ImageJ. Bars: 20  $\mu$ m.

**Fig. 7.** C2 lowers cellular VE-cadherin content.

HBMECs were grown to confluence before being exposed to 5  $\mu$ M C2. After 45 min and 3 h a cell-based ELISA (panels A, C and E) and flow cytometry analysis (panels B, D and F) were performed for evaluating the total cell content of VE-cadherin. Values are the mean  $\pm$  SD of three separate experiments, with two determinations per experiment. \*,  $p < 0.05$ ; \*\*,  $p < 0.01$ .

A and D. Where specified, cells were pre-treated with 1 mM NAC for 30 min.

B and E. Where specified, cells were pre-treated with 280 nM SU6656 for 30 min.

C and F. Where specified, cells were pre-treated with 100  $\mu$ M chloroquine for 2 h.

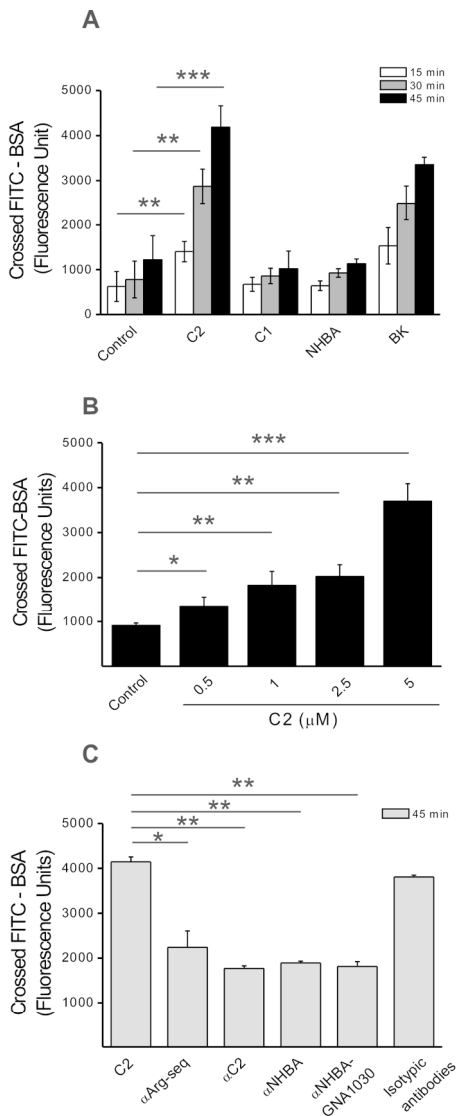


Fig. 1

Fig. 1. The C2 fragment induces the leakage of HBMECs-formed monolayer.

A. Human brain microvascular endothelial cells (HBMECs), grown as monolayer onto the membrane of a Transwell system, were stimulated with 5  $\mu$ M C2, C1, NHBA, or saline (control). 1  $\mu$ M bradikinin (BK) was used as positive control. The passage of FITC-BSA into the lower chamber, at various time intervals, was evaluated.

B. HBMEC monolayers were exposed to the indicated concentrations of C2 for 45 min. Monolayer leakage was evaluated as in A.

C. HBMEC monolayers were exposed to C2 for 45 min in the presence of the indicated antibodies. Monolayer leakage was evaluated as in A. Values are expressed as means  $\pm$  SD of duplicate determinations of four separate experiments. \*,  $p < 0.05$ ; \*\*,  $p < 0.01$ ; \*\*\*,  $p < 0.001$ .

81x192mm (300 x 300 DPI)



For Peer Review

1  
2  
3  
4  
5  
6  
7  
8  
9  
10  
11  
12  
13  
14  
15  
16  
17  
18  
19  
20  
21  
22  
23  
24  
25  
26  
27  
28  
29  
30  
31  
32  
33  
34  
35  
36  
37  
38  
39  
40  
41  
42  
43  
44  
45  
46  
47  
48  
49  
50  
51  
52  
53  
54  
55  
56  
57  
58  
59  
60

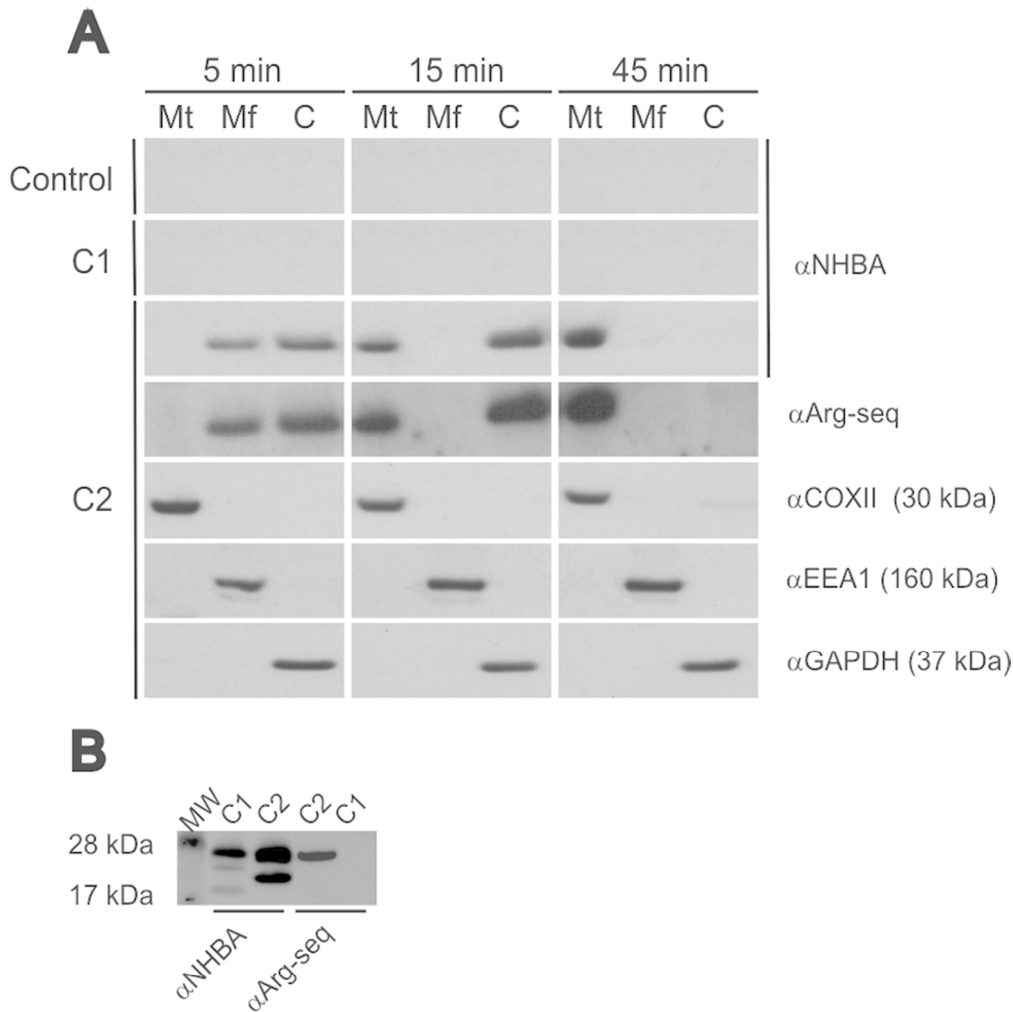


Fig. 2

Fig. 2. The C2 fragment accumulates in mitochondria.

A. HBMECs, grown to confluence in a T75 flask, were exposed to 5  $\mu$ M C2, C1 or saline (control). After 5, 15 and 45 min mitochondrial (Mt), microsomal (Mf) and cytosolic (C) fractions were isolated and processed for western blot analysis. A mouse polyclonal anti-NHBA antibody was used to reveal both C1 and C2 peptides. The latter was also revealed by a polyclonal antibody specific for the arginine-rich domain. Monoclonal antibodies anti-COXII, anti-EEA1 and anti-GAPDH were used to check the purity of each fraction. HRP-conjugated secondary antibodies were used before developing in chemiluminescence. The molecular weights of the single proteins are in brackets.

B. Control of the ability of anti-NHBA antibody to recognize the C1 peptide. 0.5  $\mu$ g of C1 and C2 were loaded in SDS-PAGE and processed for western blot as in A, using both anti-NHBA and anti-arginine sequence antibodies. The lower band of C2, not recognized by the anti-arginine sequence, is probably a degradation product of the peptide.

80x85mm (300 x 300 DPI)

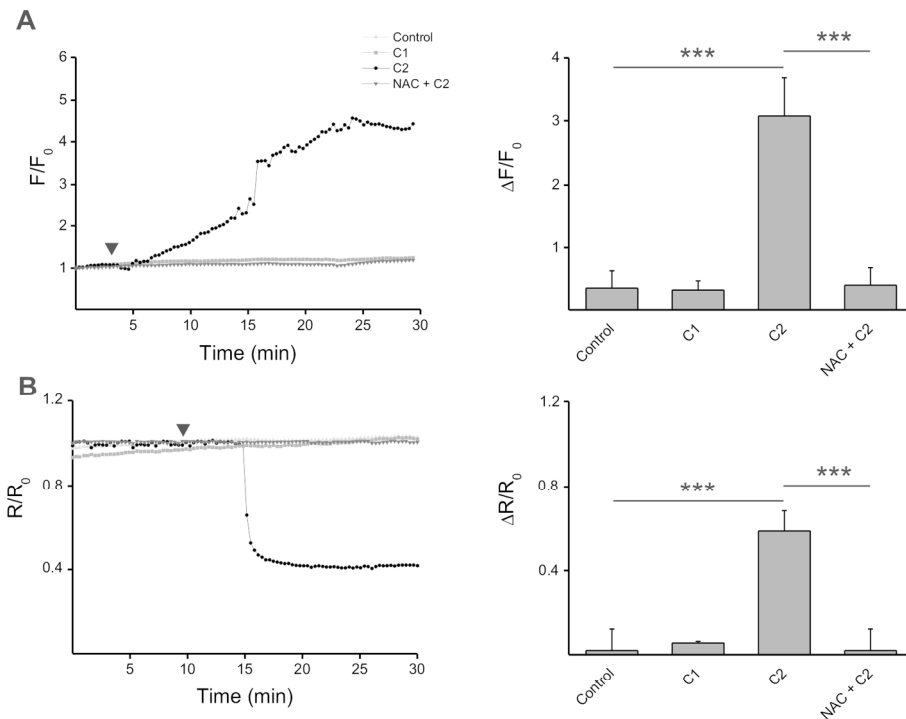


Fig. 3

Fig. 3. C2 induces mitochondrial ROS formation in HBMECs.

A. HBMECs, grown as monolayer, were loaded with 1  $\mu$ M MitoSOX Red, just before live-imaging recording.

At the indicated time point (arrow head) cells were exposed to 5  $\mu$ M C1, C2, or saline (control).

When required, cells were pre-treated with 1 mM NAC before being exposed to C2. Cells were excited by laser at 514 nm and fluorescence emitted was recorded at 560 nm every 10 s for 30 min. Data are expressed as  $F/F_0$ , where  $F$  is the fluorescence emission intensity at time  $t$  and  $F_0$  is the fluorescence emission intensity at time = 0. Each kinetics trace is the average of the recording for 3 cells and it is representative of 3 independent experiments performed on different cell preparations. The right panel reports the mean  $\Delta F/F_0 \pm$  SD for the 3 experiments, calculated at 30 min ( $N=3$  cells per experiment).

B. HBMECs, grown as monolayer, were transfected with the Hyper-dMito vector. After 24 h of expression, cells were exposed to 5  $\mu$ M C1, C2, or saline (control). When required, cells were pre-treated with 1 mM NAC before being exposed to C2. Fluorescence intensities were recorded every 10 s for 1 h. Normalized fluorescence ratio changes (420/500 nm) were calculated as a measure of H<sub>2</sub>O<sub>2</sub> production. Data are expressed as  $R/R_0$ , where  $R$  is the ratio at time  $t$  and  $R_0$  is the ratio at time = 0. Each kinetics trace is the average of the recording for 3 cells and it is representative of 3 independent experiments performed on different cell preparations. The right panel reports the mean  $\Delta R/R_0 \pm$  SD for the 3 experiments, calculated at 30 min ( $N=3$  cells per experiment). \*\*\*,  $p < 0.001$ .

158x121mm (300 x 300 DPI)

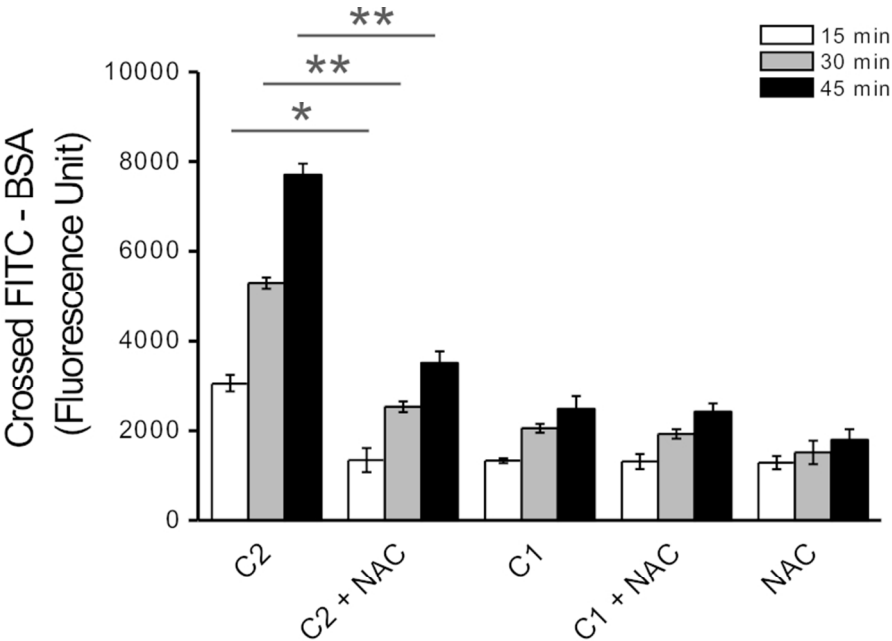


Fig. 4

Fig. 4. ROS induced by C2 are essential for the alteration of endothelial permeability. HBMECs, seeded onto the membrane of a Transwell system, were exposed to 5  $\mu$ M C2 or C1 fragment together with FITC-BSA. When required, HBMECs were pre-treated with 1 mM NAC for 30 min. The accumulation of BSA in the lower chamber was performed as detailed in Figure 1. Values are expressed as mean  $\pm$  SD of duplicate determinations of four separate experiments. \*,  $p < 0.05$ ; \*\*,  $p < 0.01$ .

79x60mm (300 x 300 DPI)

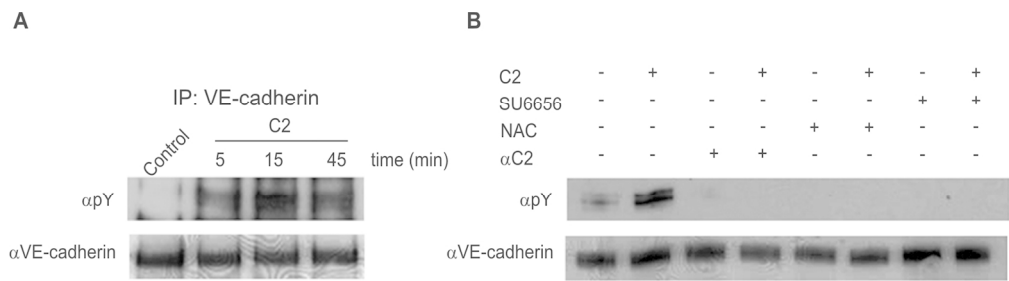


Fig. 5

Fig. 5. C2 induces VE-cadherin phosphorylation.

A. Murine endothelial cells overexpressing wild-type human VE-cadherin were grown to confluence before being serum-starved for 24 h and exposed or not to 5  $\mu$ M C2. After 5, 15 and 45 min, cells were harvested and processed for immunoprecipitation with a polyclonal antibody anti-VE-cadherin. Control is represented by cells exposed to saline for 15 min. Phosphorylation state of the protein was determined in western blot by developing with anti-phosphotyrosine antibody. Total VE-cadherin was used as loading control.

B. Cells were pre-treated or not with NAC or with the Src kinase inhibitor SU6656 for 30 min before the administration of C2. C2 was tested either as such or in the presence of anti-C2 antibodies. Control is represented by cells exposed to saline for 45 min.

140x50mm (300 x 300 DPI)

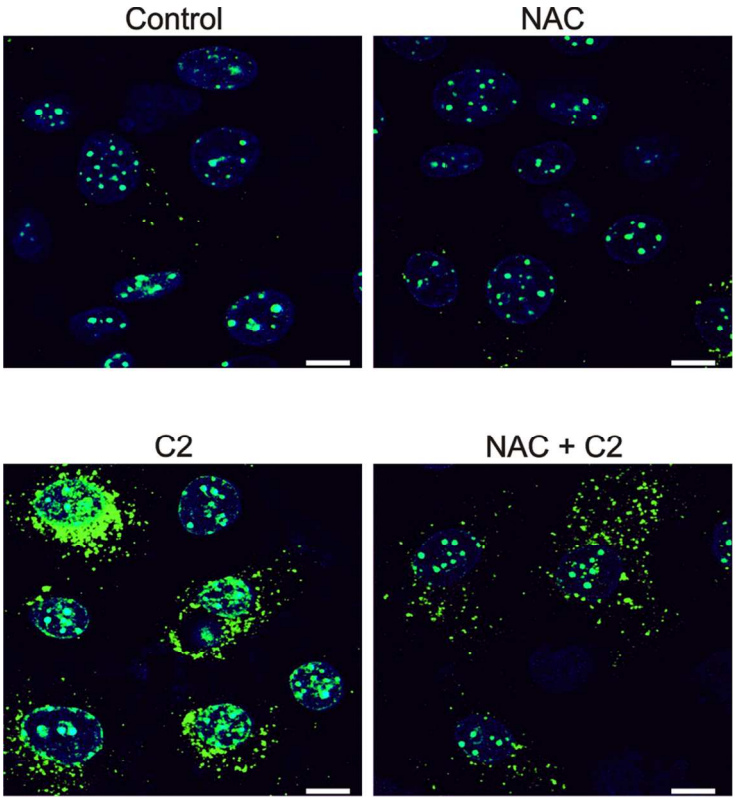


Fig. 6

Fig. 6. C2 induces VE-cadherin internalization. Murine endothelial cells overexpressing wild-type human VE-cadherin were grown to confluence. To evaluate the internalization of the cell surface-associated VE-cadherin, the junctional protein was labelled at 4°C with a monoclonal antibody specific for the extracellular domain. After C2 exposure for 45 min at 37°C, cells were processed for immunofluorescence revealing the protein-antibody complex by an appropriate secondary antibody. Where required, cells were pre-treated with 1 mM NAC for 30 min. Confocal images were acquired using a Leica microscope with a 63× oil immersion objective. Images were merged using ImageJ. Bars: 20 μm.

109x94mm (300 x 300 DPI)

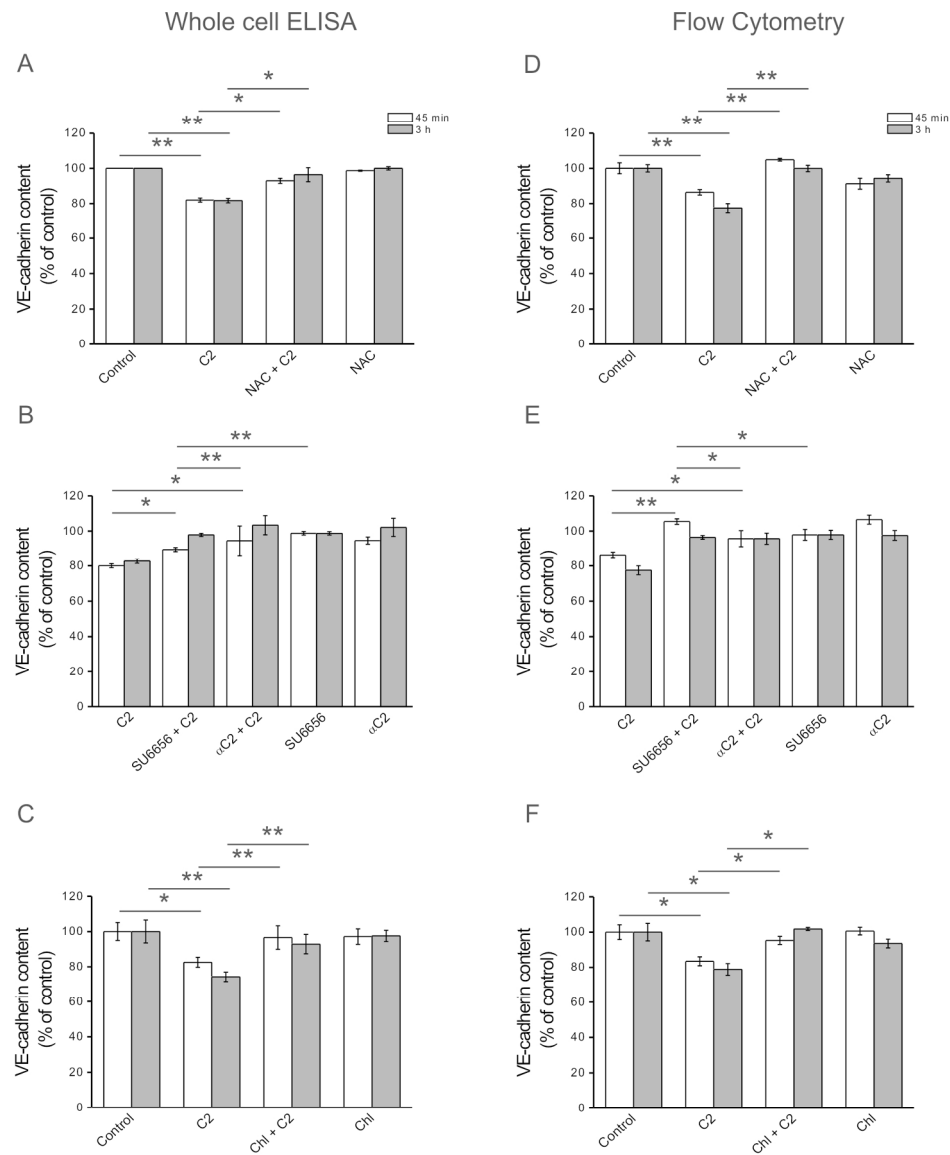


Fig. 7

Fig. 7. C2 lowers cellular VE-cadherin content.

HBMECs were grown to confluence before being exposed to 5  $\mu$ M C2. After 45 min and 3 h a cell-based ELISA (panels A, C and E) and flow cytometry analysis (panels B, D and F) were performed for evaluating the total cell content of VE-cadherin. Values are the mean  $\pm$  SD of three separate experiments, with two determinations per experiment. \*,  $p < 0.05$ ; \*\*,  $p < 0.01$ .

A and D. Where specified, cells were pre-treated with 1 mM NAC for 30 min.

B and E. Where specified, cells were pre-treated with 280 nM SU6656 for 30 min.

C and F. Where specified, cells were pre-treated with 100  $\mu$ M chloroquine for 2 h.

165x204mm (300 x 300 DPI)